Modeling and Designing the Future of Drip Irrigation: A Validated Parametric Analysis Used to Design Low Power, Pressure Compensating Drip Emitters

by

Pulkit Shamshery

M.Eng., University of Cambridge, United Kingdom (2014)

Submitted to the Department of Mechanical Engineering
in partial fulfillment of the requirements for the degree of

Master of Science in Mechanical Engineering

at the

MASSACHUSETTS INSTITUTE OF TECHNOLOGY

June 2016

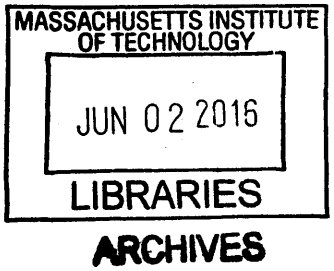

Author ..... Signature redacted
Department of Mechanical Engineering
May 20, 2016

Certified by ..... Signature redacted
Amos G. Winter, V
Assistant Professor of Mechanical Engineering
Thesis Supervisor

Accepted by ..... Signature redacted
Rohan Abeyaratne
Chairman, Department Committee on Graduate Theses

Modeling and Designing the Future of Drip Irrigation: A Validated Parametric Analysis Used to Design Low Power, Pressure Compensating Drip Emitters

by

Pulkit Shamshery

Submitted to the Department of Mechanical Engineering
on May 20, 2016, in partial fulfillment of the
requirements for the degree of
Master of Science in Mechanical Engineering

Abstract

Drip irrigation is a means of distributing the exact amount of water a plant needs by dripping water directly onto the root zone. It can produce up to 90% more crops than rainfed irrigation, and reduce water consumption by 70% compared to conventional flood irrigation. In the coming years, the demand for new, low-cost, low-power drip irrigation technology will continue to grow, particularly in developing countries. It will enable millions of poor farmers to rise out of poverty by growing more and higher value crops, while not contributing to overconsumption of water. The key inhibitor to drip adoption has been the high initial investment cost. A cost and pressure analysis revealed that a reduction in activation pressure of pressure compensating (PC) drip emitters – which can maintain a constant flow rate under variations in pressure, to ensure uniform water distribution on a field – can reduce the cost of off-grid drip systems by up to 50%. These emitter have been designed and optimized empirically in the past. In this thesis, I present a parametric model that describes the fluid and solid mechanics that govern the behavior of a common PC emitter architecture, which uses a flexible diaphragm to limit flow. The model was validated by testing nine prototypes with geometric variations, all of which matched predicted performance to within $R^2 = 0.85$. This parametric model was then coupled with a genetic algorithm to achieve a lower activation pressure of 0.15 bar for not only the 8.2 lph emitter, but also the 4, 6, 7 lph emitters. These new drip emitters, with attributes that improve performance and lower cost, are a step closer to making drip irrigation economically accessible to all throughout the world.

Thesis Supervisor: Amos G. Winter, V
Title: Assistant Professor of Mechanical Engineering

Acknowledgments

I would like to thank the following people and organizations for their contributions at different stages of my work:

- Professor Amos Winter, for his constant support, advice, technical inputs and guidance through out the course of my research; and for his drive and enthusiasm for engineering which is infectious. I would like to thank him for his patience and ability to scope high- impact projects which got me involved in a project with a reach of affecting billions of people. Thank you Amos.

- Katherine Taylor, Ruo- Qian (Roger) Wang, Dan Dorsch, Joshua Wiens and Pawel Zimoch and the rest of my fellow graduate students at MIT GEAR Lab, for their support and advice. Also thank you for contributing to the emitter work in the past.

- Abhijit Joshi and Sachin Patil of Jain Irrigation Systems Limited, for their constant guidance and support. Part funding for this project was provided by the TATA Center of Technology and Design at MIT.

- Nevan Hanumara, Chintan Vaishnav and Rob Stoner of Tata Center, for their constant feedback. Part funding for this project was provided by the TATA Center of Technology and Design at MIT.

- Friends and family, for their love, support and encouragement.

- Seema and Puneet Shamshery for their unwavering support and faith in me. Thank you, Mom and Dad. Love you both.

THIS PAGE INTENTIONALLY LEFT BLANK

Contents

List of Figures

THIS PAGE INTENTIONALLY LEFT BLANK

List of Tables

THIS PAGE INTENTIONALLY LEFT BLANK

Chapter 1

Introduction

The overall aim of this research is to design a low-cost, low-pressure, energy efficient off-grid drip irrigation system that is economically viable for small-holding farmers. This section includes the motivation for the focus of this project in terms of water scarcity, food production and security and poverty alleviation. It then presents why drip irrigation is considered to be a solution for sustainable agriculture development. The advantages and disadvantages of drip irrigation, and reasons for its poor adoption, are included.

India is the country in focus for this thesis, but it doesn't limit the impact that technological improvements in drip irrigation will have throughout the world.

1.1 Smallholder Farmers and their role in Water, Food and Economic Security

1.1.1 Food/Agriculture

There are 267 million inhabitants in India who are economically active in agriculture. This accounts for 55% of the economically active population, which is 22% of the total population [1]. If economically dependents are considered, agriculture supports 55% of India's population. Smallholder farmers (own/cultivate less than 2 ha) constitute 78% of the country's farmers [4]. They utilize 33% of the cultivated land and

contribute 41% to the nation's grain production and over half of India' s fruits and vegetables. These statistics indicate the high dependence on smallholder farmers to India's food and economic security. The dependence on smallholder farmers is even more important as the trend in India is land fragmentation and more farmers are fragmenting into the small and marginal category [5]. Agriculture contributes to 17% of India's GDP [1]. But the rate of growth in the sector has been steadily declining from 5% in 2011 to 1.1% in 2015, and this has been stated as the reason for the plateauing in the economic growth rate of India [6].

The median population in India has been estimated to reach 1.5 billion by 2025, an increase of 200 million since 2016 [7]. Food shortage might be augmented by transition in diet from grain, tuber and roots staple to more meats, fruits and vegetables, which require more irrigated water.

Numerous studies have shown a positive relationship between growth in agriculture and poverty reduction. In a cross-country study on the links between agricultural yields and poverty, it was concluded that a 10% increase in yields resulted in 5- 7% reduction in poverty [8, 9]. Agriculture's potential to reduce poverty exceeds non-agricultural activities; more than half the reduction in poverty achieved in developing countries is attributed to growth in agricultural incomes [10].

Despite their importance in national and regional food production, smallholder farmers comprise the majority of India's undernourished population and most of those living in absolute poverty [11]. Investments and advancements in agriculture is extremely important for both food security and economic growth.

1.1.2 Water

Of India's 66 million ha of cultivated land, 39% is dependent on powered irrigation (only 1.6% of which is drip irrigated) [1]. Due to inadequate water for flood irrigation and lack of rainfall, 2014-2015 was a poor year leading to a large number of crop failures and a 5.3% drop in overall grain production.

India is also the largest groundwater user in the world, with an estimated usage of around 230 cubic kilometers per year [1]. Groundwater is vital for poverty reduction

and economic growth in India, with a large fraction of the population relying on the resource directly or indirectly for livelihoods. Eighty percent of water withdrawal in India is used for agriculture and on average 63% of that comes from groundwater sources [1]. Other estimates are higher and indicate that 69% of kharif (monsoon crops) and 76% of rabi (winter crops) irrigated areas depend on groundwater [12].

Although on average India has around 430 cubic kilometers of annual replenishable groundwater resources, this average masks the large number of water stressed locations across the country, which Figure 1-1 shows graphically. On average 54% of groundwater blocks in India are over- exploited (more consumption than replenishment), for example in Gujarat, Haryana, Maharashtra, Punjab- 'the bread basket of India'- 75%, Rajasthan- 60%, Karnataka- 40% and Tamil Nadu- 40% of the groundwater blocks are over- exploited. The situation is deteriorating at a rapid pace. Between 1995 and 2004, the proportion of overexploited blocks nationwide tripled from 5 to 15 percent [12].

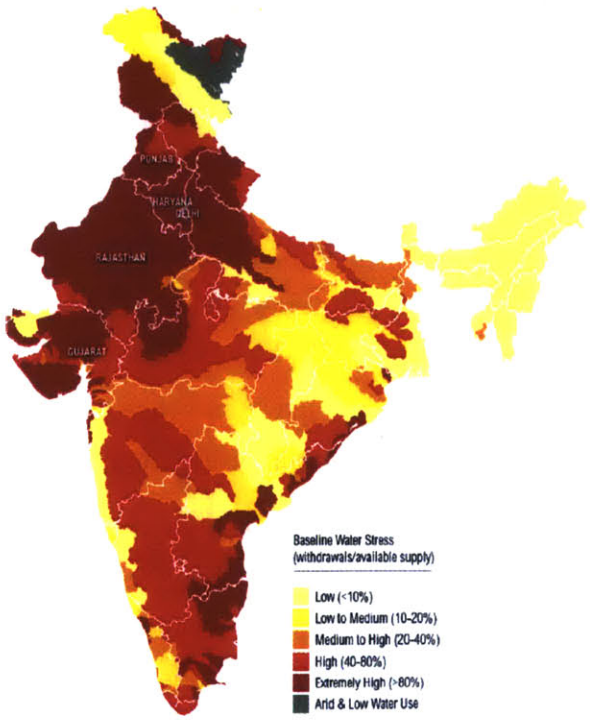

Figure 1-1: **Water Stress Index** [1]

About 15% of India's food produced in 2005 was dependent on unsustainable groundwater and that number is only increasing [13]. Overall, 25% of grain harvests have been estimated to be at risk due to groundwater depletion [14]. In the wells tested by the India Water Tool, 54% of wells showed dropped levels for seven years, with 16% declining by more than 1m/year. The most vulnerable state is Punjab. Farmers reliant on a given groundwater body result in a spiraling cycle of well deepening or redrilling and the purchase of new pump sets. This has serious social implications for the poorest, who can no longer afford such action and hence risk exclusion from irrigating their land [15].

Agriculture, being a sector that affects national food security, water security, GDP and farmer livelihoods (267 million farmers and their families), needs investment in advancements. Due to the upcoming water stresses and demand for more food, "more crop per drop" is a necessity. Drip irrigation is a suitable technology for this. Drip irrigation alone has an aggregate potential to increase revenues for India's farmers by approximately $30 billion annually if the full potential of 26 million hectares under flood irrigation in India is converted to drip [16].

1.1.3 Energy

In 2005, the government of India launched the RGGVY scheme to electrify 100% of rural India. In a report, 10 years later only 53% of rural India was electrified. In some states, spectacular progress was made while in others nothing was achieved; Andhra Pradesh (98%), Gujarat (97%), Assam (93%), West Bengal (90%), Tamil Nadu (89%) and Bihar (85%) whereas Haryana (8%), Rajasthan (27%), Odisha (34%), Karnataka (38%), and Himachal Pradesh (29%) [17]. Electricity in Gujarat and Karnataka is rationed and available for 6 hour/day whereas in Bihar it is available for less than 3 hour/day. Also India has 26 million groundwater pumps on farms, mainly diesel powered that suffer from volatile fuel costs [18].

Drip irrigation can be used to watered a farm within the available 3 hours of rationed electricity where with other irrigation techniques it is impossible. Also 47% of India being off- grid shows a serious need for off- grid drip irrigation solutions.

1.1.4 Policy and Subsidy

Subsidies currently play a major role in the adoption of drip irrigation in India. The national government provided 50% subsidy for micro-irrigation under the National Misison of Micro-Irriagtion (NMMI) which was recently extended as the Pradhan Mantri Krishi Sinchai Yojana (PMKSY) in 2016 [19]. Additional subsidies are provided by various states at the state level. In AP through the APMIP, lower caste small farmers got an additional 50% subsidy whereas the other small farmers got 40% and other farmers got no additional state subsidy [20]. Government of Tamil Nadu, provides small farmers with an additional subsidy of 50% and others get 25% [21]. Government of Punjab provides a flat 25% additional subsidy to all farmers up to an area of 5 ha per beneficiary [22]. In Gujarat, The Gujarat Green Revolution Company (GGRC) is responsible for subsidy distribution. It provides an additional 20% to small farmers, 10% to others and 35% to lower caste farmer's up to a cost limit [23].

Despite the availability of high subsidies, less than 0.1% farmers receive these annually and subsidies only end up going to farmers with political connections. Hence a low-cost drip system is essential to make drip irrigation economically accessible without the reliance on subsidies.

1.2 Motivation for Drip Irrigation

Droughts, climate change, erratic rainfall, diminishing groundwater, limited and erratic power supply coupled with poverty have compelled farmers to look for a technology that would enable them to irrigate their crops within these constraints. A low-cost conventional drip system is required.

1.2.1 Advantages of Drip Irrigation

The commonly stated advantages of drip irrigation are: Drip irrigation, compared to rain fed and flood irrigation, can increase yields by 20-90% depending on crop type, save water consumption per acre by 30-70%, reduce fertilizer usage per acre by up to

40%. Drip irrigation also allows the farmers to grow water sensitive cash crops such as floriculture and horticulture crops [24–27].

In areas like north Gujarat and Kolar where water is actually bought at a price from a neighboring well (ranging from Rs.1.5/m^3 to Rs.2.5/m^3 in north Gujarat to Rs.6/m^3 in Kolar) [28], water savings have such a huge impact that these areas were early adopters of drip irrigation.

Other advantages include labor savings, less weeding and pests . Drip irrigation can also be used with saline water [28].

In India electricity is usually rationed and is provided for a short duration. Hence with flood irrigation, a portion of the land has to be left fallow as the duration of energy is insufficient to irrigate the complete area but this issue is resolved with drip as all the land receives approximately equal water at all times. In some hard rock areas such as Maharashtra, MP, AP and Karnataka especially in Kolar, the dug tube wells have poor yields. The farmer needs to discontinue irrigation every hour for 2-3 hours for the well to recuperate hence reducing the command area that can be covered with flood irrigation due to electric rationing. With drip and its significant water savings, the command area is increased, hence increasing capacity and yields for smallholder farmers [29]. Table 1.1 presents the advantages concisely in a tabular form.

1.2.2 Disadvantages of Drip Irrigation

The commonly stated disadvantage of drip irrigation is the constant clogging issue in emitters where water is hard and irrigation management is poor. Also drip irrigation is not robust to allow for crop changes as it is designed and optimized for one cropping pattern. Other issues are rodents eating through the pipes, hooves breaking pipes, and over-pressurization leading to bursting pipes.

Table 1.1: Advantages of drip irrigation

Production and Socio- Economic benefits
Water savings of 30-70% compared to flood irrigation.
Yield increases of 20-90% compared to flood and rain- fed irrigation.
Ability to grow water sensitive crops
40% savings in fertiliser usage
Less weeding required
Lower labour requirement
Less pesticide usage
Greater irrigated area with same amount of water
Uniformity of water distribution on sloping land
Socio- Cultural benefits
Poverty reduction
Drip irrigation confers the image of a progressive farmer
Ecological benefits
Improved water use efficiency - lowers groundwater exploitation
Less pesticide usage

1.2.3 Lack of Drip Adoption

Despite the advantages of drip irrigation and its potential in economic benefit for smallholder and water saving potential, drip has not been a commercial success in India. Drip irrigation in India accounts for 1.6% of the irrigated land, significantly lower than the 21% in the USA and 80% in Israel [30].

The constraints to adoption of drip irrigation can be classified into physical, agronomical, socio-economic, financial, institutional-pricing, subsidies and policy related. These also provide adequate explanation for the high levels of adoption in other parts of the world.

In terms of financial reasons, a drip irrigation system costs $1000 an acre and an additional $3000 for solar if the water comes from a surface source (41% of irrigated land). The capital investment is too large for most farmers to afford and others to consider. Even huge subsidies (50% national level to additional state subsidies of up to 40%) is only making it accessible for few farmers. The lack of a financial institution to support farmers during this high risk investment is a significant inhibitor for adoption.

Also expensive service/ maintenance and spare parts have been commonly cited as inhibitor to adoption [31].

The physical reason is a lack of independent water source and pump. Also if the farmer relies on surface canal water, there is mismatch in water delivery and irrigation schedule, some farmers get water every 10-15 days at very low pressures; unsuitable for drip irrigation, which requires constant delivery of water [28].

In terms of socio-economic reasons, a lack of well-defined water rights and subsidized or free electricity provide no incentive for most farmers to save water or electricity [29]. Savings don't result in any private gains, making drip irrigation less attractive as an investment. But in the district of Kolar in Karnataka, due to lack of ownership of wells farmers have to buy water from neighbors and this has incentivized many local farmers to investment in drip for its water and fertilizer saving while increasing yields [28]. It has also been noted that more educated, knowledgeable and trained farmers tend to adopt drip before the rest [32].

In terms of agronomical reason, drip is more suitable for row crops than field crops. Drip is great for horticulture, wide spaced crops but the returns only ramp up after 3 years of investment, which is too long a wait for smallholder household [33]. Farmers opting for wider spaced horticulture or floriculture crops have been the early adopters of drip in all states [32]. It should also be noted that a drip system designed for one crop in unsuitable for another, this inhibits farmer from rotating their crops.

In terms of subsidy reasons, an insufficient knowledge of subsidies and poor administration is pushing away farmers from applying to subsidies. Also a non-transparent selection process is inhibiting farmers from applying. In states (APMIP and GGRC) where there has been an attempt at improvements in administration of subsidies, namely farmers pay in full and get subsidies in return, have seen a significant adoption in drip; 30,000 ha within one year of creation. This also allows the drip irrigation market to behave like a free market where all companies have a fair chance and this leads to greater R&D and reduction in prices of drip.

Chapter 2

Drip Irrigation

Drip irrigation is a highly water-efficient method of irrigation. Drip irrigation refers to a system where water is pumped through a network of filters, pipes and emitter to deliver regulated flow directly to the plant root zones. Figure 2-1 shows a typical drip irrigation setup.

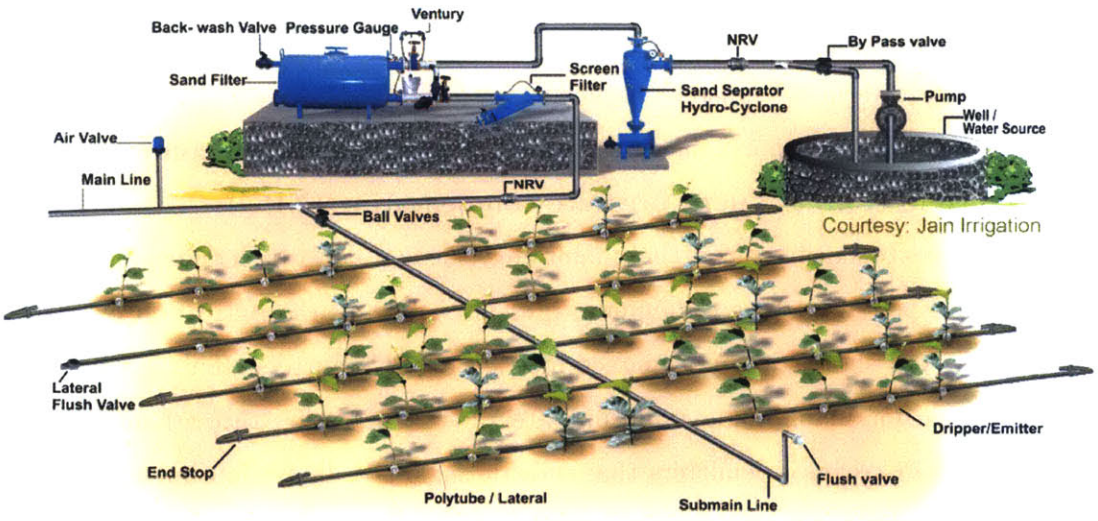

Figure 2-1: **Typical Drip Irrigation System** (Photo courtesy: Jain Irrigation)

2.1 Components

The main components of a Drip System are (see Figure 2-1):

1. **Pump (centrifugal (most common))**

   Pump water out of a water source which is usually a surface source (river or a canal) or groundwater source and then pressurize the water to pump it through the drip piping system.

2. **Filters (Screen, Sand, Disc and Hydro-Cyclone)**

   These remove the sediments and precipitates within the water in order to reduce emitter clogging

3. **Pipes (Main, Sub-Main and Lateral)**

   The piping network conveys the water so that it can be emitted in a controlled manner directly near the plant root zone.

4. **Valves** which include Flush, Non return, By Pass, Air and Ball Valves.

5. **Emitter**

   These are devices that control the flow of water out of the piping network and into the plant root zone.

   They can be divided into two subgroups (see Figure 2-2): **Inline emitters** are molded directly into the tubing and tend to be cheaper. **Online emitters** are installed on the outside of irrigation tubing and tend to give more flexibility to farmers in terms of emitter placement.

   Each dripper group can be further subdivided into **pressure compensating emitters (PC)** and **non- pressure compensating (NPC)**.

   PC refers to a drip emitter that maintain a constant flow rate independent of the applied pressure above a minimum pressure known as the Activation pressure. Figure 2-3 shows the performance metric of a PC emitters. This attribute is valuable for maintaining uniform water flow distribution throughout a farm field. NPC refers to emitters that provide some flow limitation but not to the extent of PC emitters (see Figure 2-3).

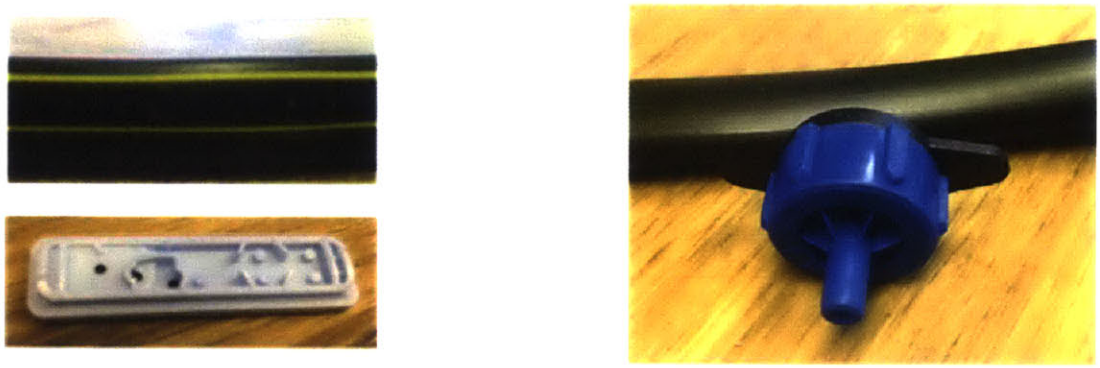

Figure 2-2: **Left: Inline emitter; Right: Online emitter**

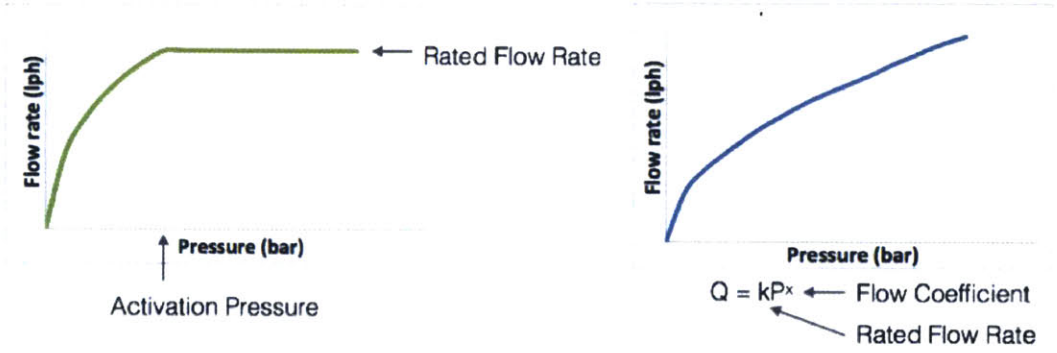

Figure 2-3: **Pressure Compensating and Non Pressure Compensating emitter**

2.2 Cost Analysis

As mentioned in section 1.2.3, the major inhibitor to the widespread adoption of drip irrigation system is the high initial cost. A cost analysis was performed on a representative one-acre field under drip. Table 2.1 lists the assumptions made during this cost analysis. The price list for the different drip system components was obtained from the Gujarat Green Revolution Company (GGRC) [23].

Figure 2-4 shows the cost breakdown of the drip system under several emitter scenarios. A closer look (Figure 2-5) reveals that approximately 80 - 86% of the cost

Table 2.1: Assumptions made during cost analysis

Plant	Banana
Farm size	1 acre
Emitter and Lateral spacing	1 metre
Total number of emitters	4000/acre
Emitter flowrate	8 lph
Pump	25% efficiency and hypothetical
Lateral diameter	12 mm
Submain diameter	63 mm
Scenario	Off- grid solar
Water Source	Surface water

for drip systems with either PC 1 bar activation pressure or NPC emitters stems from the powering and pumping system. A reduction in the cost of these systems will result in a significant reduction of the cost of the overall off- grid drip system.

$$Power = \textbf{Pressure} * Flowrate \tag{2.1}$$

Equation 2.1 shows that to reduce the power requirement of the system, the pumping pressure and flow rate through the system need to be reduced. The flow rate is controlled by the crop water requirement and the duration of pumping time and can only be lowered if the duration of pumping is extended. Therefore to reduce the pumping requirement for a constant pumping duration, the pressure loss through the system has to be reduced.

2.3 Pressure loss Analysis

A pressure loss analysis was performed on the system described in Table 2.1. The emitter selected was an online PC emitter with a 1 bar activation pressure. It should be noted that the pressure loss analysis is representative of the inline PC emitter at 1 bar activation pressure and the NPC emitter too. Table 2.2 shows the pressure drops along the drip irrigation system. The majority of the pressure loss is in the emitter;

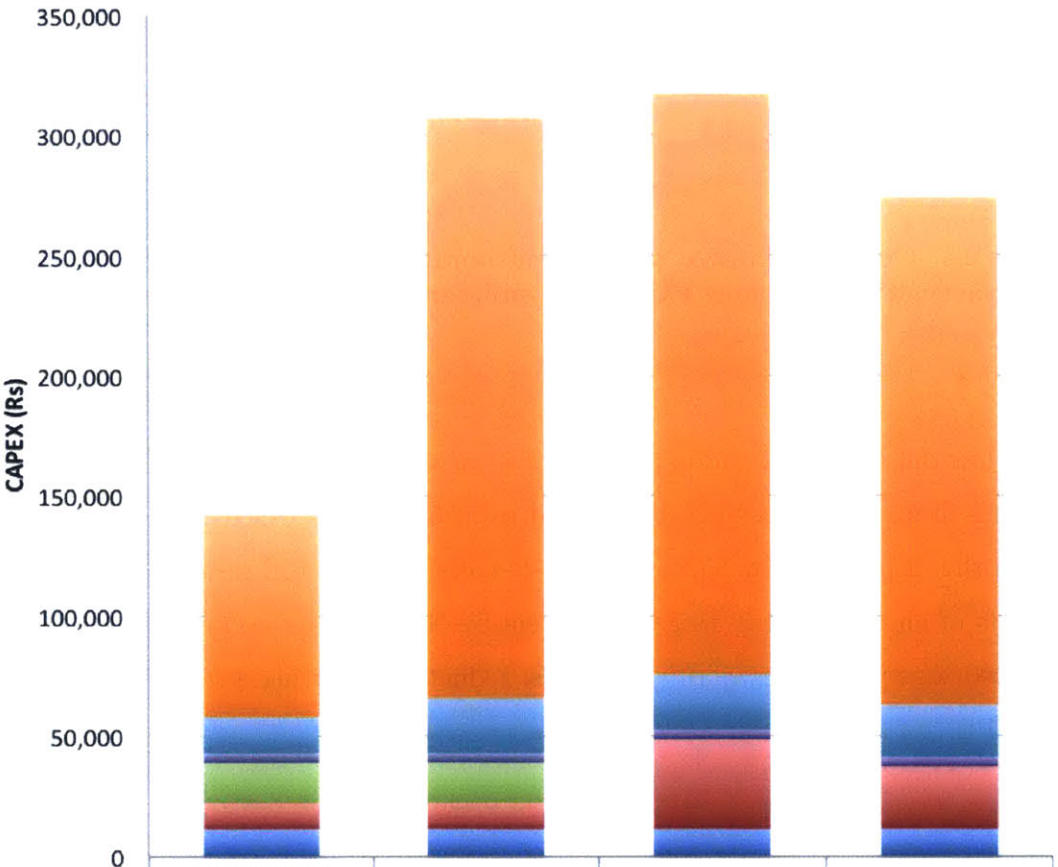

	PC (0.15 Bar) Online	PC (1 Bar) Online	PC (1 Bar) Inline	NPC
Solar	84,223	241,617	241,617	211,010
Pump	14,912	22,856	22,856	21,539
Submain	3,952	3,952	3,952	3,952
Lateral	16,633	16,633	0	0
Dripper	10,724	10,724	37,136	25,749
Filter	11,551	11,551	11,551	11,551

Figure 2-4: **Cost breakdown under different emitter scenarios**

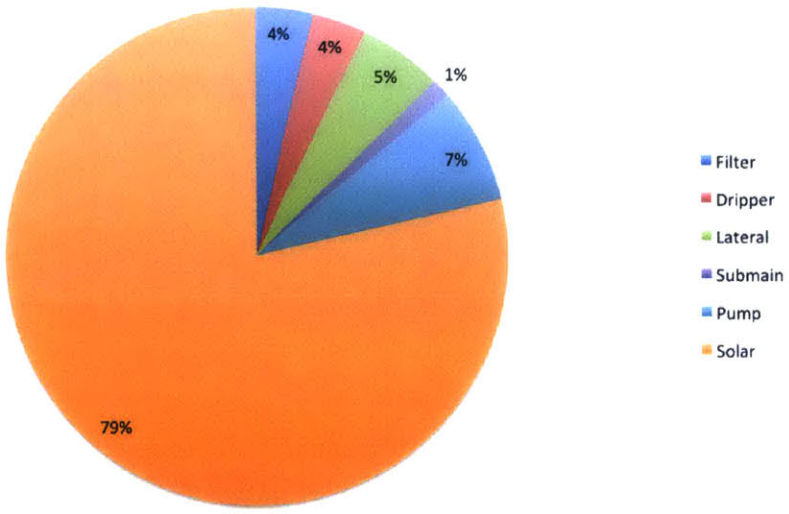

Figure 2-5: **Cost breakdown of different components of a drip system for a 1 bar activation pressure PC online emitter**

it the loss due to the activation pressure of 1 bar which accounts for 64% of the total pressure drop. If this loss can be reduced to 0.15 bar, this will reduce the pressure loss in the drip system by 55%. Figure 2-4 shows that this will result in a reduction in costs of an off-grid drip irrigation system by 50% from an average of \$4000/acre to \$2000/acre with the majority of the cost reduction occurring due to the reduction in CAPEX of solar panels.

Table 2.2: Pressure loss analysis

	Pressure Drop (Bar)	**Percentage (%)**
Filter	0.20	13
Piping and Valves	0.35	23
Emitter	1.00	64
Total Losses	1.55	100

2.4 Drip Irrigation Emitters

As has been discussed in Section 2.3, a reduction in activation pressure for a PC emitter from the current 1 bar to 0.15 bar will result is a 50% cost reduction compared to not only the 1 bar PC emitter scenarios but also the NPC emitter scenario (see Figure 2-4). The focus of this master's thesis is to analyze the coupled fluid-structure interaction within a pressure compensating (PC) drip emitter and experimentally validate this analysis. This validated analysis is valuable because it will provide key insights into the sensitivities of the geometric and material variables to lower activation pressure. This model can then be coupled with a single objective genetic algorithm (GA) to try realizing geometries that can achieve lower activation pressure.

2.4.1 Design Requirements

In order to make drip irrigation a significantly more affordable and attractive option for small-holder farmers, the following design requirements must be met.

1. The emitters must exhibit PC behavior to ensure uniform water delivery throughout the field. This means that, within a certain range, regardless of the pressure differential applied across the emitter, the emitter must passively deliver a constant flow rate (see Figure 2-6).

2. The emitters must exhibit an activation pressure of 0.1-0.3 bar, which is the main factor that will allow for the system to become affordable as a solar-powered or on grid irrigation system. This reduction in activation pressure is what makes PC drip systems more economically accessible than NPC systems (see Figure 2-6).

3. A family of emitters ranging from 3-20 litres per hour with a low activation pressure must be realised (see Figure 2-6).

4. The emitters must also be robust enough to withstand handling in the field. This means that they should not clog easily and must have a reasonable lifetime

of around 5 years. That is the emitters should be at par or better in clogging performance than existing emitters.

5. The manufacturing constraint is that currently used injection-molding machines should be able to be cost-effectively retrofitted to manufacture the new emitters.

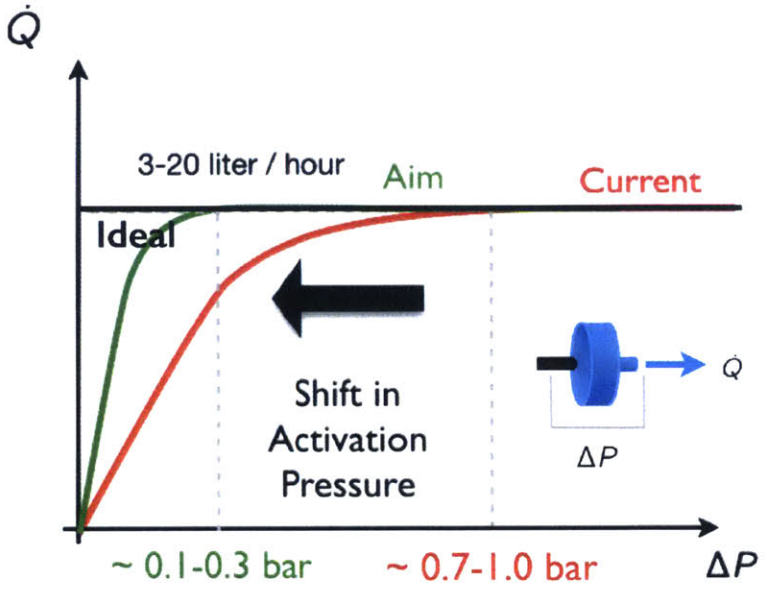

Figure 2-6: **Flow control performance of a PC drip emitter.** The red line shows the behavior of a commercially available PC dripper [2], which was used as the benchmark in this study. The vertical dashed line shows the "activation pressure": the minimum pressure required for the dripper to achieve its rated flow rate. The green line represents the targeted performance curve. The black line is the theoretical ideal performance

2.4.2 Prior Art

W. G. Miller 1947 - Flow Control Device

The Flow control device, patented in 1947 (see Figure 2-7), is cited as the first flow limiting device. The working principle of this flow controller is similar to currently manufactured emitters. A compliant membrane sits on top of a channel through which water flows out. As pressure increases, the membrane deflects into the channel

in shear increasing the flow resistance and resulting in flow controlling behavior. This aspect of design is surprisingly similar to the architecture of currently manufactured emitters.

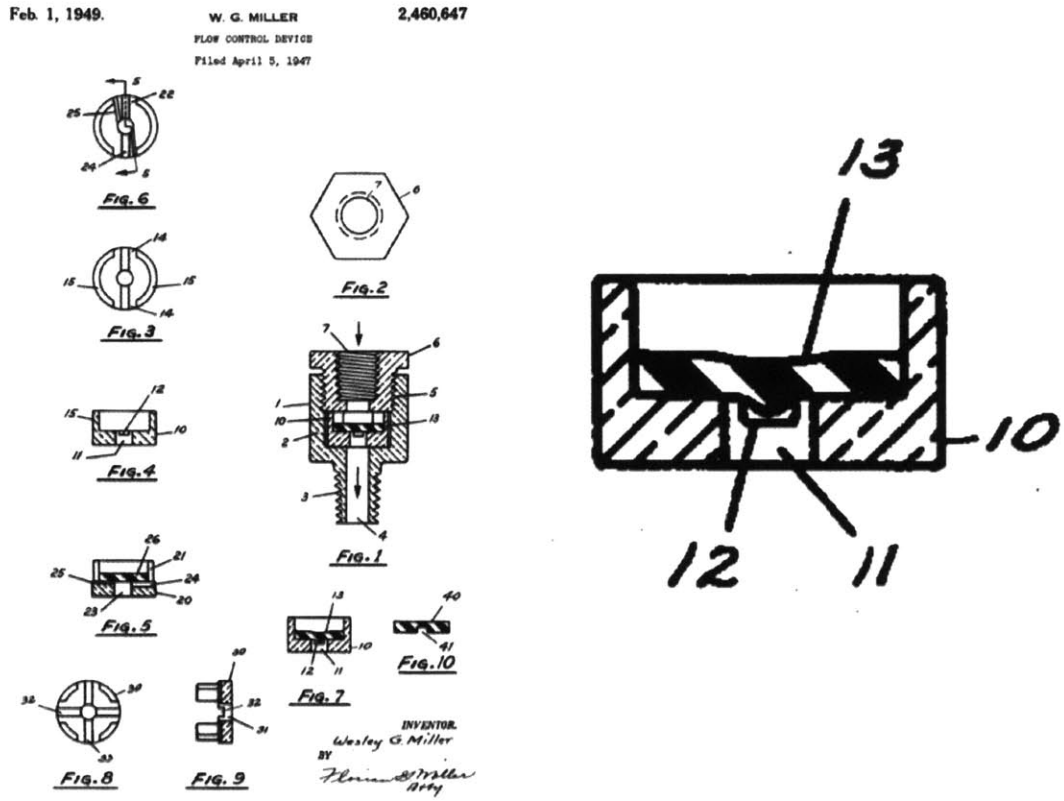

Figure 2-7: **Flow Control Device Patent from 1947** This is cited as the first emitter. The working principle of this device is very similar to existing devices [3].

Currently Manufactured Online emitters

The currently manufactured emitter design is guided by designers' intuition and iterative experimentation, or by computer aided emulation. These methods make optimization a very time consuming and computationally expensive process.

The 8.2 lph manufactured by Jain Irrigation was used as the benchmark point for the parametric analytical model. Figure 2-8 shows the family of Jain emitters.

Figure 2-8: **Jain Online emitters** This is the family of online emitters manufactured by Jain [2].

Chapter 3

Multidisciplinary Optimization

3.1 Problem Formulation

The overall objective of this study is to reduce the activation pressure of online emitters. The starting point of the analysis is the currently manufactured Jain 8.2 lph online emitter. Figure 3-1 shows the design variables considered during this optimization.

$$\begin{aligned} x_1 &= \text{membrane radius } (r_m) \\ x_2 &= \text{membrane thickness } (t) \\ x_3 &= \text{channel width } (W) \\ x_4 &= \text{channel length } (L_{ch}) \\ x_5 &= \text{channel depth } (D_{ch}) \\ x_6 &= \text{land height } (H_l) \\ x_7 &= \text{orifice size } (A_{orifice}) \\ x_8 &= \text{outlet diameter } (D_o) \end{aligned} \tag{3.1}$$

The fluid-structure interaction is modeled as a function whose inputs are the described set of design variables and parameter and the output is the emitter performance. Here, the emitter performance is characterized using the goodness-of-fit of the inlet pressure vs. flow rate graph of the emitter to the aimed performance (see

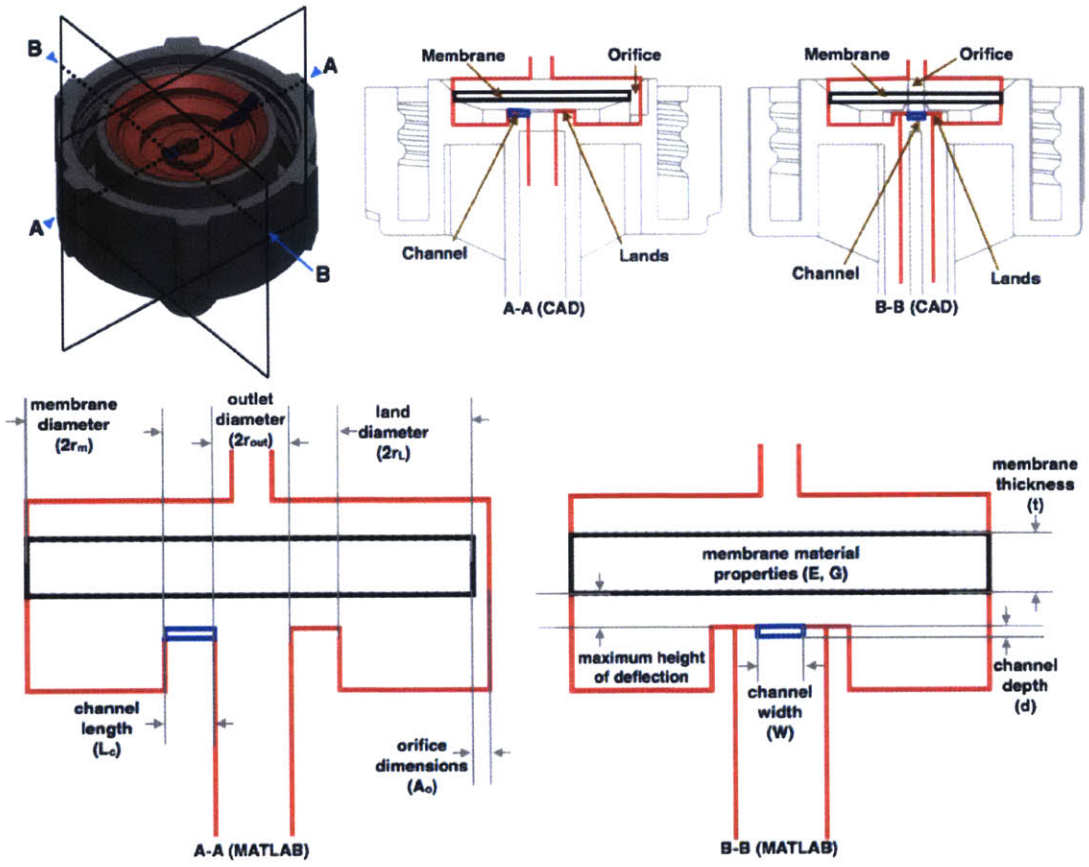

Figure 3-1: **Schematics of a conventional pressure compensating online drip emitter which uses a flexible membrane to control flow rate.** A: Isometric view showing the section planes. B: Half-cut view on the A-A plane. C: Orthogonal view to the channel, cut on the B-B plane. D: MATLAB modeled schematic corresponding to the cut view on the A-A plane. E: MATLAB modeled schematic corresponding to the cut view on the B-B plane. D and E show the critical dimension of the flow features within the dripper which were used to model its behavior.

Figure 2-6). The flow rate versus pressure graph for an ideal emitter is a horizontal line at the required flow rate (shown in black in Figure 2-6) and this was set as the target for the optimization problem. It should be noted that the aimed graph (shown in green in Figure 2-6) is a more realistic graph that can be achieved due to practical considerations resulting from the fact that the orifice loss coefficient (k_0) can never be zero. Therefore, the objective of the optimization problem amounts to determining the set of design inputs that minimize the deviation between the inlet pressure vs. flow rate performance of the designed emitter and the aimed performance (see Figure 3-2).

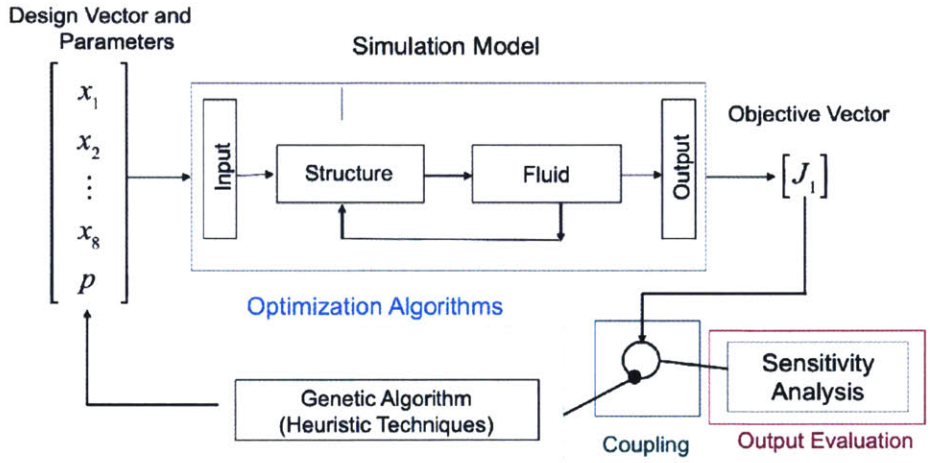

Figure 3-2: **Problem Formulation** Design variables are the inputs into the simulation module which outputs the cost function (the Euclidean distance between the designed and aimed performance). A hybrid genetic algorithm is then used to minimize the cost function. The GA is coupled with key learning from sensitivity analysis to guide the design and optimization process.

The mathematical representation of this objective is shown in Equation 3.2. The deviation between the curves (cost function) is measured as the Euclidean distance between the vector of corresponding graph points between the designed and the aimed performance.

$$J_1 = \sum_{i=1}^{n} \| q_i^{aimed} - q_i^{design} \| \tag{3.2}$$

Here,

J_1 = Objective (cost) function

n = total number of discretization of the operating pressure range

q_i^{aimed} = aimed flow rate at i^{th} pressure discretization

q_i^{design} = design flow rate at i^{th} pressure discretization

A genetic algorithm (GA) based heuristic optimization method was used to minimize the objective function given in equation 3.2. A GA based approach was preferred over other optimization techniques because the objective function is noncontinuous and contains non-linear constraints and GA are well suited for this forms of design space. Additionally, GA's are well suited for handling integer constraints. This is necessary in order to take into account the dimensional tolerances while injection molding the emitter. The constraints enforced are due to manufacturing and procurement constraints are detailed in Equations 3.3. The manufacturing constraint results from the requirement that currently used injection-molding machines should be able to be cost-effectively retrofitted to manufacture the new emitters. This enforces the following dimensional constraints (g and h):

$$\begin{aligned}
g_1 = 1.2 &\leq \text{membrane thickness } (mm) \leq 1.4 \\
g_2 = 10 &\leq \text{membrane diameter}(mm) \leq 14 \\
g_3 = 0.05 &\leq \text{Land Height } (mm) \leq 1 \\
g_4 = 0.05 &\leq \text{channel depth } (mm) \leq 1 \\
g_5 = 0.5 &\leq \text{channel width } (mm) \leq 2 \\
g_6 = 0.5 &\leq \text{channel length}(mm) \leq 2 \\
g_7 = 0.5 &\leq \text{area of orifice } (mm^2) \leq 2 \\
h_1 = &\text{Young's Modulus } (GPA) = 0.038 \\
h_2 = &\text{Shear Modulus } (MPA) = 0.60 \\
h_3 = &\text{Poisson Ratio} = 0.48 \\
h_4 = &\text{Membrane Material} = \text{silicone}
\end{aligned} \tag{3.3}$$

The GA optimization toolbox in MATLAB was used for the optimization process.

Values for the population size, mutation rate, and crossover rate were iteratively tuned for optimal emitter design while keeping the computation inexpensive.

3.2 Working principle of PC Emitters

The working principle of an online emitter is that fluid flows into the emitter through the inlet at pressure P_1. The fluid then flows into the chamber under the membrane through an orifice. The flow through the orifice leads to a pressure loss and the pressure in the chamber is at P_2. The fluid then flows out of the emitter to the atmosphere at pressure P_a. The flow of fluid creates a pressure differential across the membrane. As the inlet pressure increases, the compliant membrane deflects down to the lands and then further shears into the channel. The overall deflection increases with inlet pressure, resulting in more fluid flow resistance. This flow restriction behavior is graphically summarized in Fig. 3-3.

3.3 Fluid Structure Interaction

The analysis of an emitter involves coupled fluid-structure interactions (FSI). The fluid flow is dependent on the deflection of the membrane, while the pressure loading which causes the membrane deflection is dependent on the fluid flow. Numerical methods to solve FSI can be divided into either segregated or monolithic [34–37]. In this study, a segregated solver was used in which the fluid and solid problems were solved separately while exchanging information at their boundaries. As flow in the emitter is assumed to be steady, segregated solvers can take advantage of modularity, hence use known solutions for both the solid and fluid domains and then couple them through fixed-point iteration. Figure 3-4 graphically depicts the iterative process used in this study to converge the FSI. The output of the iteration was an inlet pressure versus flow rate curve for different geometries and materials.

For every inlet pressure P_1 applied to the emitter, an initial pressure loading of $P_2 = P_a$ was assumed. The membrane deflection was then calculated using this

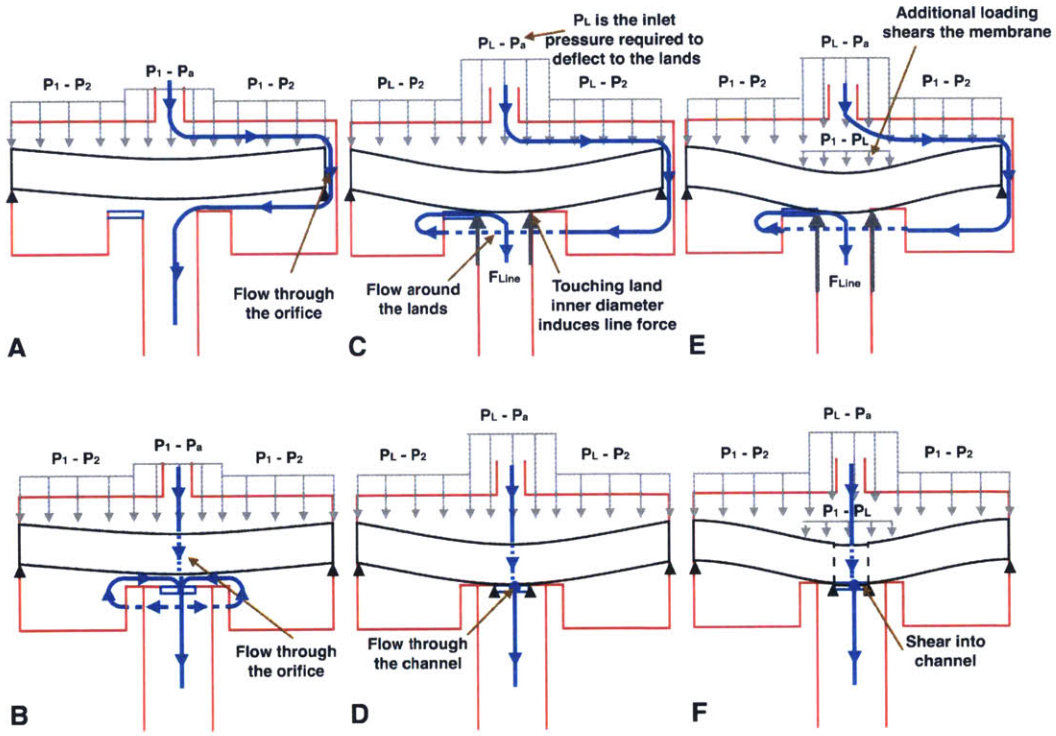

Figure 3-3: **Graphical summary of the working principle of a drip emitter.** A and B: Bending of the flexible membrane shown in the A-A and B-B planes from Fig. 3-1A, respectively. C and D: Line force contact between the membrane and the lands, shown in the A-A and B-B planes from Fig. 3-1A, respectively. E and F: Deflection of the membrane into the channel from shearing, shown in the A-A and B-B planes from Fig. 3-1A, respectively. The flow path of water is shown by connected blue arrows. Gray arrows denote the pressure differential acting on the membrane. Bold arrows denote the contact force at the edge of the land, F_{Line}. The black triangles show constraints to membrane deflection.

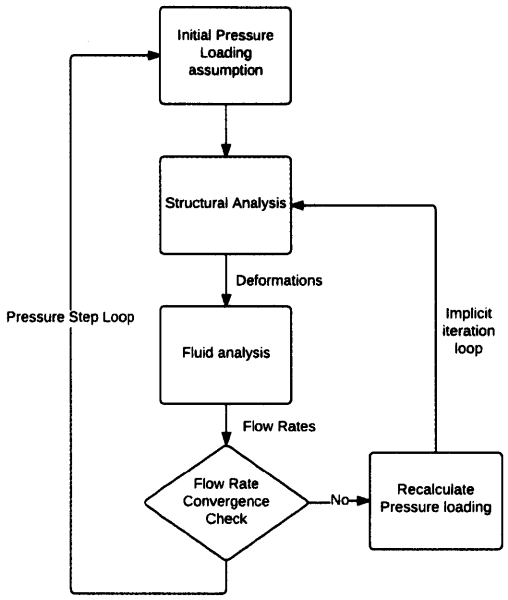

Figure 3-4: **Flow diagram for the process used to model the coupled fluid and solid mechanics behavior within a drip emitter.**

pressure loading. The resulting membrane deflection defined the flow path through the emitter and was used to determine the resulting flow rate, Q_{i}. Finally, Q_{i} was used to recalculate P_2 with

$$P_2 = P_1 - \frac{1}{2}\rho\left(\frac{Q_i}{A_0}\right)^2 \kappa_0, \tag{3.4}$$

where k_0=0.95 was the experimentally measured loss coefficient for the orifice in the 8 l/hr benchmark emitter used in this study, A_0 was the orifice area, and ρ is the density of water. In each iteration, the recalculated P_2 yielded new values for membrane deformation and flow rate. This process was repeated until the new predicted flow rate and the flow rate calculated in the previous iteration converged to within 0.5%. Once the flow rate at a certain inlet pressure was determined, a new inlet pressure was assumed. This iterative process was repeated at each inlet pressure to build up the entire flow rate versus pressure profile for the dripper.

3.3.1 Structural Deformation Modelling

The deformation of the circular membrane can be characterized by three regimes. As the inlet pressure is increased, first the compliant membrane deforms in bending up to the lands (Figs. 3-3 A and B). The membrane then contacts the lands and seals the channel (Figs. 3-3 C and D). Finally, it deforms in shear into the channel (Figs. 3-3 E and F).

Deformation in Bending The small deflection in bending, w, was given by the solution of the fourth order partial differential equation [38]

$$\Delta^4 w = \frac{q}{D}, \tag{3.5}$$

where

$$D = \frac{Et^3}{12(1-\nu^2)} \tag{3.6}$$

and q is the pressure loading, D is the flexural stiffness of the membrane, E is the young's modulus, t is the thickness and ν is the poisson ratio of the membrane. The assumed pressure loading is shown in Figs. 3-3 A and B. The circular membrane was assumed to be thin and simply-supported along the outer edge. These boundary conditions reflect that the membrane can physically move radially while supporting rotation along the edge.

Because the geometry of and loading on the membrane are axisymmetric, the spatial coordinate can be simplified to 2D, perpendicular and transverse to the circular plate. The deflection due to loading in Figs. 3-3 A and B can be calculated by assuming the deflections as small and linear. They are determined by superimposing the deflection of a circular plate due to uniform loading from P_1- P_a, and the deflection due to annular loading from P_2- P_a. The exact analytical solutions for these loadings are known and given by [38]. Deflection of a circular plate due to uniform loading is

$$w_{uniform} = (P_1 - P_a)\frac{r_m^4}{64D}\left(1 - \left(\frac{r}{r_m}\right)^2\right)\left(\frac{5+\nu}{1+\nu} - \left(\frac{r}{r_m}\right)^2\right), \tag{3.7}$$

where r_m is the membrane radius and r is a spatial position in the radial direction. Deflection of circular plate due to annular loading is

$$w_{annular} = -(P_2 - P_a)\frac{r_m^4}{2D}\left(\frac{L_{17}}{1+\nu} - 2L_{11}\right) + \frac{(P_2 - P_a)r_m^2 L_{17} r^2}{2D(1+\nu)} - \frac{(P_2 - P_a)r^4 G_{11}}{D}, \tag{3.8}$$

where for r < r_p

$$G_{11} = 0, \tag{3.9}$$

and for r > r_p

$$G_{11} = \frac{1 + 4\left(\frac{r_p}{r}\right)^2 - 5\left(\frac{r_p}{r}\right)^4 - 4\left(\frac{r_p}{r}\right)^2\left(2 + \left(\frac{r_p}{r}\right)^2\right)\log\left(\frac{r}{r_p}\right)}{64}. \tag{3.10}$$

For all r

$$Y_c = -\frac{(P_2 - P_a)r_m^4}{2D}\left(\frac{L_{17}}{1+\nu} - 2L_{11}\right), \tag{3.11}$$

$$M_c = (P_2 - P_a)r_m^2 L_{17}, \tag{3.12}$$

$$L_{17} = \frac{1 - \frac{1-\nu}{4}\left(1 - \left(\frac{r_p}{r_m}\right)^4\right) - \left(\frac{r_p}{r_m}\right)^2\left(1 + (1+\nu)\log\left(\frac{r_m}{r_p}\right)\right)}{4}, \tag{3.13}$$

$$L_{11} = \frac{1 + 4\left(\frac{r_p}{r_m}\right)^2 - 5\left(\frac{r_p}{r_m}\right)^4 - 4\left(\frac{r_p}{r_m}\right)^2\left(2 + \left(\frac{r_p}{r_m}\right)^2\right)\log\left(\frac{r_m}{r_p}\right)}{64}, \tag{3.14}$$

where r_p is the radial position of the start of the distributed annular loading and is

equivalent to half way between the lands ($(r_{out} + r_L)/2$). G_{11} is a function of the radial location r and the start of annular loading r_p. Y_c is the center deflection and M_c is the center moment. L_{11} and L_{17} are loading constants dependent on the ratio of r_p/r_m. The total deflection is the summation of the two loadings,

$$w_{bending} = w_{uniform} + w_{annular}. \tag{3.15}$$

Equations (3.7) to (3.15) are valid for small deflections (maximum deflection, $w_{max} <$ thickness of membrane, t). Once the deflections exceed the thickness of the plate, induced radial stresses cause the plate to stiffen, and the deflection is no longer proportional to the magnitude of the loading.

Timoshenko derived a correction that accounts for the stiffening effect, which can be multiplied by the small deflection to give a good estimate of the actual deflection [39]. The correction factor is

$$\frac{w_{max,large}}{t} + 0.262\left(\frac{w_{max,large}}{t}\right)^3 - \frac{w_{max,small}}{t} = 0, \tag{3.16}$$

$$w_{bending,large} = w_{bending,small}\left(\frac{w_{max,large}}{w_{max,small}}\right), \tag{3.17}$$

where $w_{max,large}$ is the maximum large deflection, and is dependent on the thickness of the membrane and the maximum small deflection for a loading, $w_{max,small}$.

Deformation while Interacting with the Lands Once the membrane deflects to the lands, an opposing circular line force is induced to prevent the membrane from deflecting further (Figs. 3-3 C and D). This line force is due to the contact of the membrane on the inner diameter of the lands. The magnitude of the force is derived by employing the boundary condition that the membrane can not deflect further than the lands. The pressure required to cause the membrane to deflect to the lands is labelled P_L.

Deformation in Shear Once the membrane deflects to the lands, the pressure loading P_1 - P_L will result in additional membrane deflection in shear into the channel (Figs. 3-3 E and F).

As only a small section of the plate shears into the channel, the deflection can be approximated as the shearing deformation of a simply supported thick beam. The deflection is given by [40].

$$w_{shear} = \frac{3}{5}\frac{(P_1 - P_L)W^2}{GA_b}\left(\frac{x}{W} - \frac{x^2}{W^2} - \frac{2}{(\lambda W)^2}\left(1 - \frac{\cosh(\lambda x - \lambda\frac{W}{2})}{\cosh(\lambda\frac{W}{2})}\right)\right), \quad (3.18)$$

where

$$\lambda^2 = \frac{\beta}{\alpha}; \alpha = \frac{B_0}{A_0} - A_0; \beta = \frac{GA_bC_0}{EIA_0}, \quad (3.19)$$

$$A_0 = \cosh\left(\frac{1}{2}\right) - 12\left(\cosh\left(\frac{1}{2}\right) - 2\sinh\left(\frac{1}{2}\right)\right), \quad (3.20)$$

$$B_0 = \cosh^2\left(\frac{1}{2}\right) + 6\left(\sinh(1) + 1\right) - 24\cosh\left(\frac{1}{2}\right)\left(\cosh\left(\frac{1}{2}\right) - 2\sinh\left(\frac{1}{2}\right)\right), \text{ and} \quad (3.21)$$

$$C_0 = \cosh^2\left(\frac{1}{2}\right) + \frac{1}{2}\left(\sinh(1) + 1\right) - 4\cosh\left(\frac{1}{2}\right)\sinh\left(\frac{1}{2}\right). \quad (3.22)$$

In Eqs. 3.19-3.22, G is the shear modulus of the membrane, A_b is the cross-sectional area of the beam, W is the length of beam and width of channel, and x is the spatial position. Constants A_0, B_0 and C_0 appear in the coupled Euler-Largrange governing differential equations of a thick beam deforming in bending and shear [40].

3.3.2 Fluid Flow Modelling

The numerical method used to model the flow is correlation; exact eddy simulation and flow visualization is unnecessary. The two main regimes of flow which result in major pressure losses are the flow through the orifice (Fig. 3-5 A) and through the channel (Fig. 3-5 B).

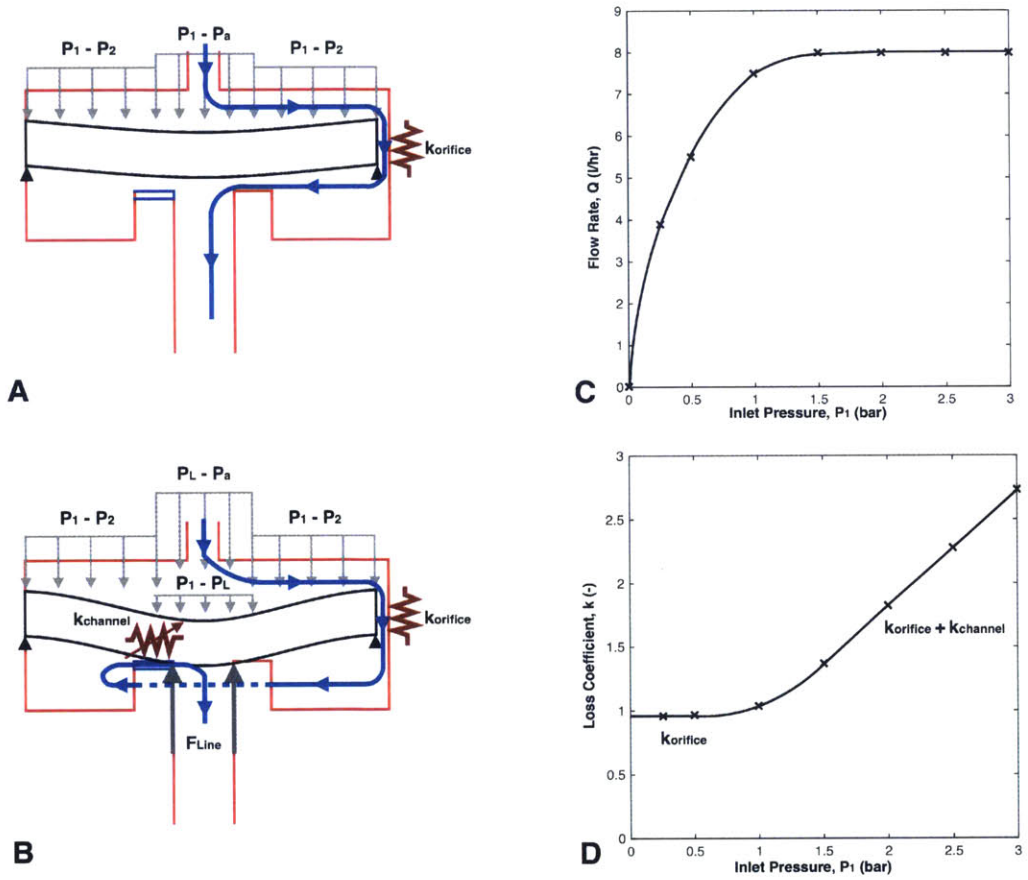

Figure 3-5: **Fluid flow modeling through an 8 l/hr drip emitter.** A: Bending of the flexible membrane under initial loading, cut in the A-A plane shown in Fig. 3-1A. The primary flow restriction in this case is caused by $k_{orifice}$, shown by a resistor symbol and plotted in the first section of Fig. 3-5D. B: Shearing of the flexible membrane into the channel, cut in the A-A plane shown in Fig. 3-1. Flow restriction is caused by the sum of $k_{orifice}$ and the variable resistance (shown by the variable resistor symbol) of $k_{channel}$, which increases with rising inlet pressure as shown in Fig. 3-5D. C: Flow rate versus inlet pressure for pressure compensating behavior. D: Loss coefficient in the fluid network versus inlet pressure.

Pressure Loss through the Orifice The pressure drop due to the orifice is calculated by

$$\Delta P_{orifice} = P_1 - P_2 = Q^2 \left(\frac{1}{2} \frac{\rho}{A_{orifice}^2} \kappa_{orifice} \right), \tag{3.23}$$

where $k_{\text{orifice}} = 0.95$ is the experimentally obtained loss coefficient value for the orifice of a 8 l/hr benchmark emitter used in this study.

Pressure Loss through the Channel Studies [41–44] have shown that the pressure drop within a channel with length scales of the order of hundreds of microns can be evaluated using macro-scale formulae. Hence the pressure drop and flow rates through the channel can be expressed by

$$\Delta P_{channel} = P_2 - P_a = \frac{1}{2} \rho \frac{Q^2}{A_{channel}^2} (\kappa_{inlet} + \kappa_{friction} + \kappa_{outlet}). \tag{3.24}$$

This is rearranged to give

$$\Delta P_{channel} = Q^2 \left(\frac{1}{2} \frac{\rho}{A_{channel}^2} (\kappa_{inlet} + \frac{fL}{D_h} + \kappa_{outlet}) \right), \tag{3.25}$$

where

$$D_h = \frac{4A_{channel}}{p_{channel}} \text{ is the equivalent hydraulic diameter} \tag{3.26}$$

and A_{channel} is the area of the channel, p_{channel} is the perimeter of the channel, f is the friction factor, r is the fluid density, Q is the volumetric flow rate through the emitter, L is the effective length of channel (i.e. the length of channel fully) and k_{inlet} and k_{outlet} are the minor loss coefficient due to inlet and exit from the channel whose values can be obtained from Kays and London [45].

The friction factor for laminar flow (i.e. for $Re_{\text{D}_\text{h}} < 2300$) can be calculated as

$$f = \frac{N}{Re_{D_h}}, \tag{3.27}$$

where N is dependent on the cross-sectional aspect ratio [46]. For $Re_{\text{D}_\text{h}} > 2300$ (i.e.

assumed turbulent flow), the friction factor can be calculated using the Colebrook equation despite the non-circular cross section [47],

$$\frac{1}{\sqrt{f}} = -2\log_{10}\left(\frac{\epsilon}{3.7D_h} + \frac{2.51}{Re_{D_h}\sqrt{f}}\right), \tag{3.28}$$

where ϵ is the roughness of the flow path and the flow is usually in the turbulent regime.

The flow rate can be calculated using Eqs. (3.24)-(3.28) and mass continuity for incompressible fluids. Using this calculated flow rate, the pressure loading can be recalculated and the iteration described in Fig. 3-4 can be repeated.

Total Pressure Loss through the Emitter In the Structure Deformation subsection, it was noted that the deformation of the circular membrane is split into three regimes. These three regimes result in two distinct flow paths through the emitter (Fig 3-3). When the inlet pressure is low and in the regime of bending the membrane down to the lands, the major pressure losses occur within the orifice, given by

$$\Delta P_{total} = P_1 - P_a = \Delta P_{orifice} = Q^2\left(\frac{1}{2}\frac{\rho}{A_{orifice}^2}\kappa_{orifice}\right). \tag{3.29}$$

When the inlet pressure increases and the deflection transitions to shearing the membrane into the channel, the major losses occur within the orifice and also the channel, causing a total pressure drop of

$$\Delta P_{total} = P_1 - P_a = \Delta P_{orifice} + \Delta P_{channel} = Q^2\left(\frac{1}{2}\frac{\rho}{A^2}\kappa_{total}\right) \tag{3.30}$$

$$= Q^2\left(\frac{1}{2}\frac{\rho}{A_{orifice}^2}\kappa_{orifice} + \frac{1}{2}\frac{\rho}{A_{channel}^2}(\kappa_{inlet} + \frac{fL}{D_h} + \kappa_{outlet}\right). \tag{3.31}$$

3.3.3 Explanation of PC Behaviour

Equations (3.29) and (3.31) summarize how the the flow rate is dependent on the inlet pressure. Figure 3-5D provides insight into the fact that to achieve pressure-

compensating behavior, the loss coefficient, k_{total}, needs to vary linearly with the increase in inlet pressure.

Figure 3-5D shows two trends. Before the pressure compensating regime, the loss coefficient k_{total} is approximately constant at 0.95, which is the experimentally measured value of k_{orifice}. This confirms that before the membrane touches the lands, the major pressure losses occur due to flow restriction through the orifice. Pressure compensation begins when the flexible membrane shears into the channel, creating an additional increase in the overall resistance by adding the variable resistance k_{channel}.

Equation (3.31) can be rewritten as

$$\Delta P_{total} = Q^2 \left(K_{orifice} + K_{minor} + K_{friction} \right), \tag{3.32}$$

where

$$K_{orifice} = \frac{1}{2} \frac{\rho}{A_{orifice}^2} \kappa_{orifice}, \tag{3.33}$$

$$K_{minor} = \frac{1}{2} \frac{\rho}{A_{channel}^2} (\kappa_{inlet} + \kappa_{outlet}), \text{and} \tag{3.34}$$

$$K_{friction} = \frac{1}{2} \frac{\rho}{A_{channel}^2} \frac{fL}{D_h}. \tag{3.35}$$

As water can be considered an incompressible fluid, K_{minor} can be assumed to be constant. Assuming the friction factor f does not change significantly in the turbulent regime, Eq. (3.32) shows that for the emitter to exhibit pressure compensating behavior, K_{friction} needs to increase linearly with pressure. For K_{friction} to increase, the effective length of channel needs to increase (Fig. 3-6 A), and the hydraulic diameter and cross-sectional area of the channel needs to decrease (Fig. 3-6 B). These effects vary in combination to achieve a linearly increasing K_{friction}, and thus pressure compensation with increasing input pressure.

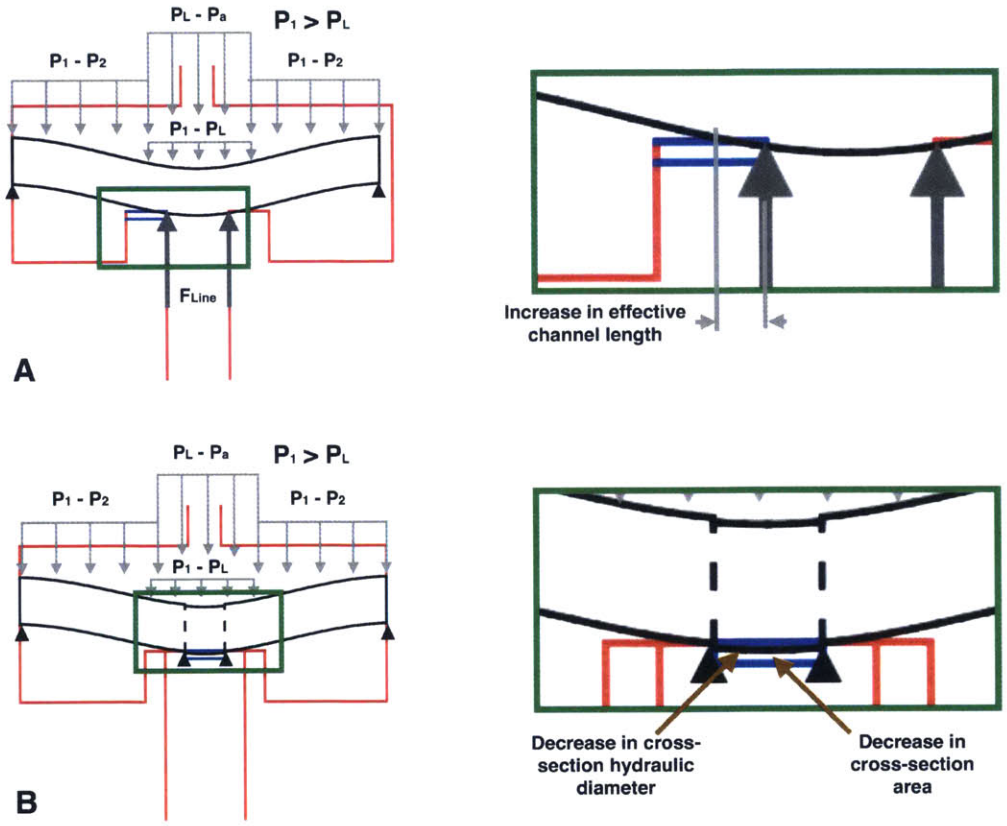

Figure 3-6: **Mechanics that yield pressure compensating behavior and a linear increase in the total loss coefficient.** A: Bending of flexible membrane under loading, cut in the A-A plane. Increases in inlet pressure causes the flexible membrane to deflect further and cover up a larger length of the channel. This results in an increase in effective length of the flow path as shown in the inset of Fig. 3-6 A (The black membrane covers up more of the blue channel). B: Shearing of the flexible membrane into the channel, cut in the B-B plane. Increases in inlet pressure causes the flexible membrane to shear further into the channel which leads to a decrease in cross-sectional hydraulic diameter and area of the flow path as shown in the inset of Fig. 3-6 B (The black membrane deflects into the blue channel reducing the effective flow path area and hydraulic diameter).

Chapter 4

Results and Discussion

4.1 Validation of Model

4.1.1 Experimental Setup

The experimental setup used to validate the theoretical model developed in the previous section is shown in Fig. 4-1. The setup is a scaled-down version of the apparatus used to characterize drip emitter behavior in industry, as well as the setup described in the ITRC technical report 2013 [48]. This similarity ensures that the data collected is comparable to data available for commercial emitters. The setup consists of a air-pressurized tank that provides water at a prescribed inlet pressure, which can be read off the pressure gauge. The pressure-regulating valve enables the control over the prescribed pressure. This setup allows for two emitters to be tested simultaneously and the emitters flow into a 250 ml graduated cylinder, which enables the flow rate to be timed.

4.1.2 Experimental Protocol

The experimental protocol used followed the Indian Standard for Irrigation Equipment and Emitter Specification [49]. The performance metric of emitters is the flow rate versus inlet pressure graph. Hence, the experimental setup should be capable of reproducing the pressure versus flow rate graph for every emitter being tested. For

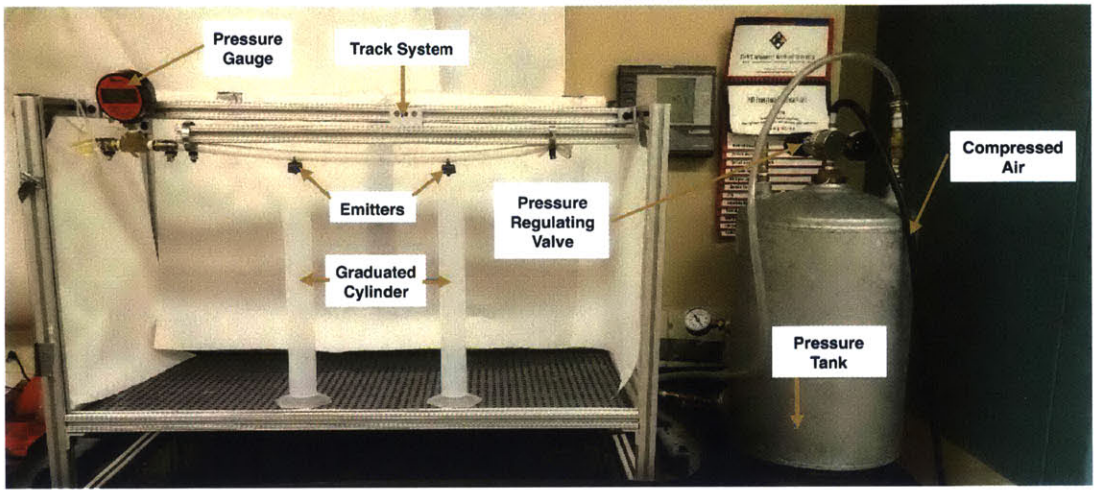

Figure 4-1: **Experimental setup used to test drip emitters**. The inlet pressure was controlled by regulating compressed air that was fed into a tank of water, which was then connected to the emitters. Flow rate was determined by measuring the time to fill 250 ml graduated cylinders. Two drip emitters can be tested simultaneously.

this, we tested two emitters of each type. The test starts an initial pressure of 0.2 bar which is set using a pressure regulating valve. At each subsequent pressure, the time taken to fill up a 250 ml graduated cylinder is recorded and the flow rate derived. The average flow rate of both emitters is plotted. The test is repeated at increasing pressures intervals of 0.1 bar up to a maximum pressure of 1.6 bar. We also repeated the tests with decreasing pressures from 1.6 bar to 0.2 bar in interval of 0.1 bar.

4.1.3 Parameter Change

In order to obtain experimental results and validate our theory, at least two drip emitters each, for eight different geometric configurations, were precision machined from delrin using a CNC milling machine. The geometric conditions changed are those shown in Fig. 3-1 D and E. Table 4.1 shows the dimensions of the six different emitters. Emitter 1 is a close replica of the currently manufactured 8 l/hr dripper that was used as a benchmark in this study but with a deeper channel. Emitter 1 served as the control. Emitters 2 and 3 only varied in channel depth. Emitter 4 varied in channel width, emitter 5 varied in deflection height, emitter 6 is varied in channel

length. Emitter 7 varies in both channel depth and deflection height whereas emitter 8 varies in channel depth and channel width. Due to the involved testing routine a parameter study design of experiments was opted for over a full factorial. The four key variables namely: channel depth, channel width, channel length and deflection height were varied one at a time with each factor having two/ three levels. Emitters 7 and 8 were introduced to capture interaction between variables.

Table 4.1: Dimensions for the eight emitters tested in this study

	Emitters (mm)							
Parameter	**1**	**2**	**3**	**4**	**5**	**6**	**7**	**8**
Channel Depth	**0.30**	**0.35**	**0.45**	0.3	0.3	0.3	**0.25**	**0.15**
Channel Width	**1.20**	1.20	1.20	**1.40**	1.20	1.20	1.20	**1.00**
Channel Length	**2.40**	2.40	2.40	2.40	**4.80**	2.40	2.40	2.40
Max Deflection	**0.70**	0.70	0.70	0.70	0.70	**0.00**	**0.30**	0.70
Outlet Diameter	**1.90**	1.90	1.90	1.90	1.90	1.90	1.90	1.90
Membrane Diameter	**11.00**	11.00	11.00	11.00	11.00	11.00	11.00	11.00
Membrane Thickness	**1.20**	1.20	1.20	1.20	1.20	1.20	1.20	1.20

Emitter 1 is the control. The bold and underlined values denote the changes made to the respective emitters when compared to the control.

4.1.4 Experimental Data Compared to Model Predictions

First and most importantly, comparing the datasheet for Jain 8.2 lph emitter and theorectical predictions shows a very close correlation (Figure 4-2). The R^2 value was 0.91 and the model was accurately able to predict the activation pressure and very closely able to reproduce the rated flow rate.

In the flow rate versus inlet pressure results for the tested prototypes, each emitter is represented by three lines. Cross markers represent the averaged results of the two emitter tests under increasing pressure repeated five times, while the circle markers represent the averaged results of the two emitters under decreasing pressure repeated five times. The solid line is the theoretical prediction. It should be noted that under higher pressures, our experimental prototypes leaked slightly, which contributed to the slightly higher flow rates than predicted.

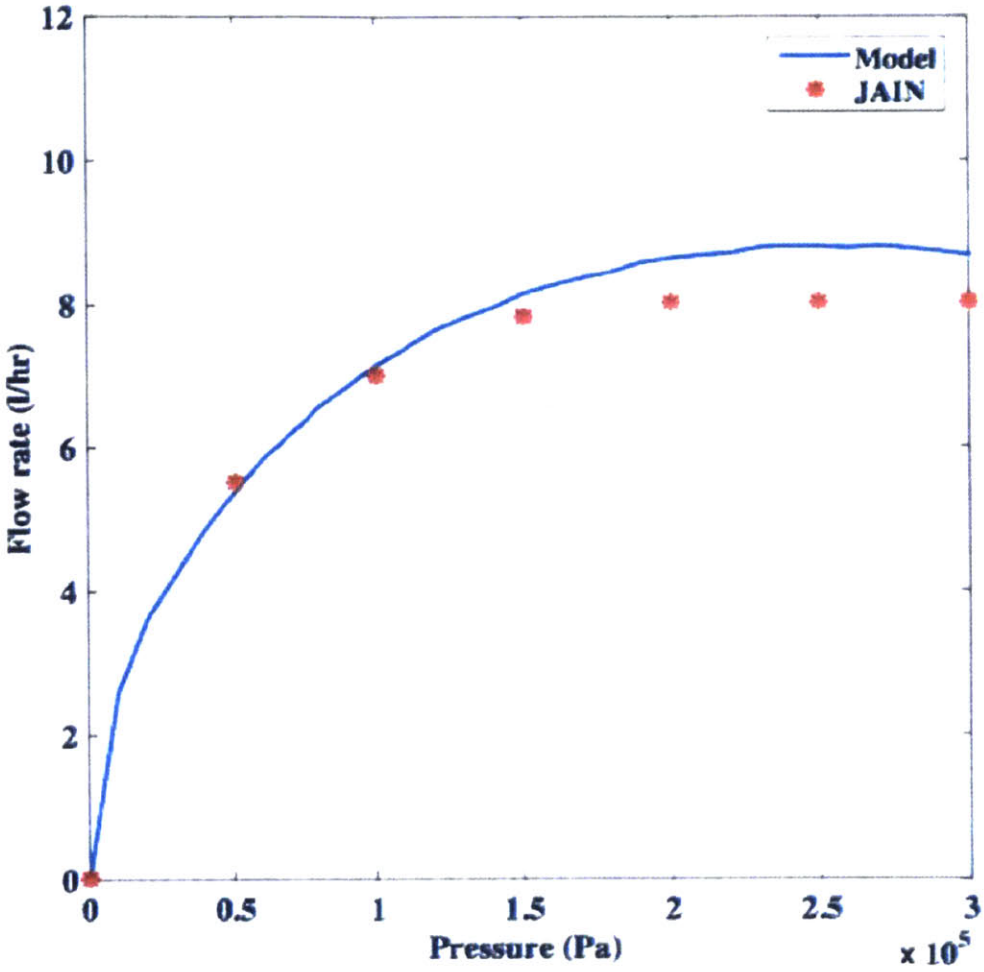

Figure 4-2: **Flow rate versus inlet pressure.** Comparing the Jain's published data (red markers) to Model's prediction (blue line).

Depth of Channel Figure 4-3 shows a close correlation between the experimental data and theoretical predictions for differing channel depths. For emitters 1, 2 and 3, the R^2 value was 0.94, 0.96 and 0.91, respectively. The trend seen is that an increase in channel depth led to increased flow rates. An increase in channel depth will make the cross-sectional area greater without affecting the deflection of the membrane, leading to a decrease in flow resistance and higher flow rate. This trend is commonly seen in currently manufactured emitters where lower flow rate emitters have a shallower channel, while higher flow rate emitters have deeper channels [2, 50].

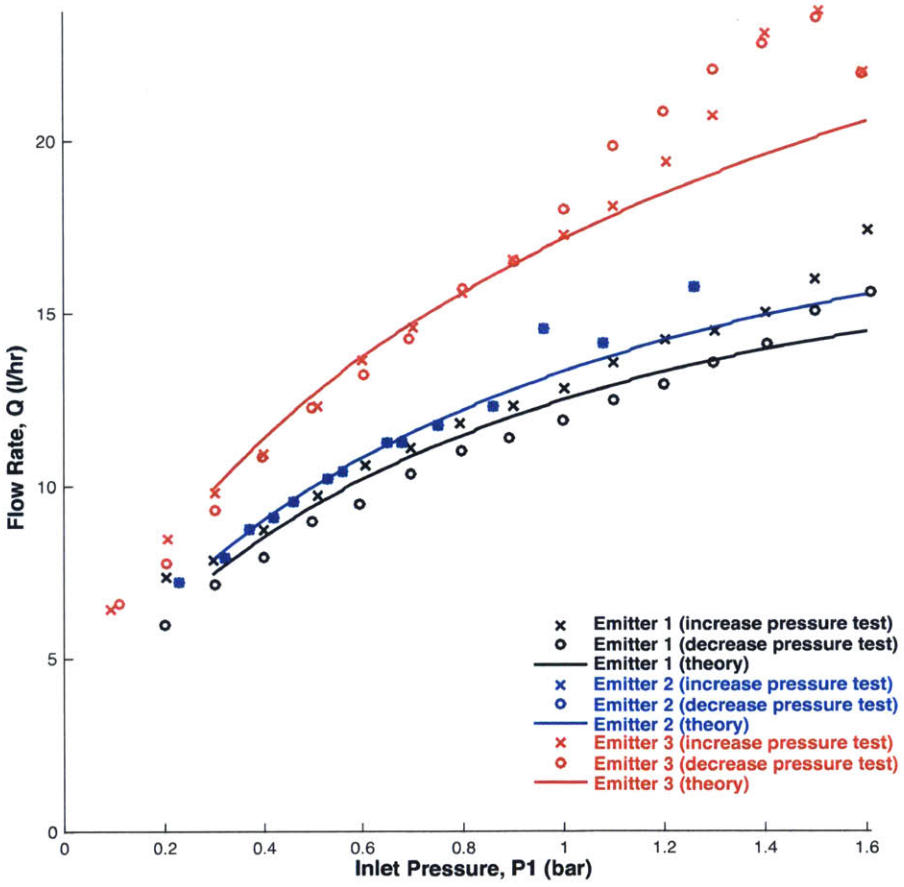

Figure 4-3: **Flow rate versus inlet pressure with variations in channel depth.** Two CNC milled emitters were tested simultaneous, and the tests repeated five times for increasing and decreasing pressures tests. The plotted results are averages from the 10 data set each.

Width of Channel Figure 4-4 shows a close correlation between the experimental data and theoretical predictions for differing channel widths. Emitter 4 has a R^2 value of 0.90. The trend seen is that an increase in channel width led to a decrease in flow rate, especially at higher inlet pressures. An increase in channel width facilitates larger deflection of the membrane in shear, which counteracts the increase in area. Flow resistance due to an increase in shear deflection dominates over the decrease in resistance due to a larger initial cross-sectional area of the channel, resulting in a net increase in resistance and lower flow rate.

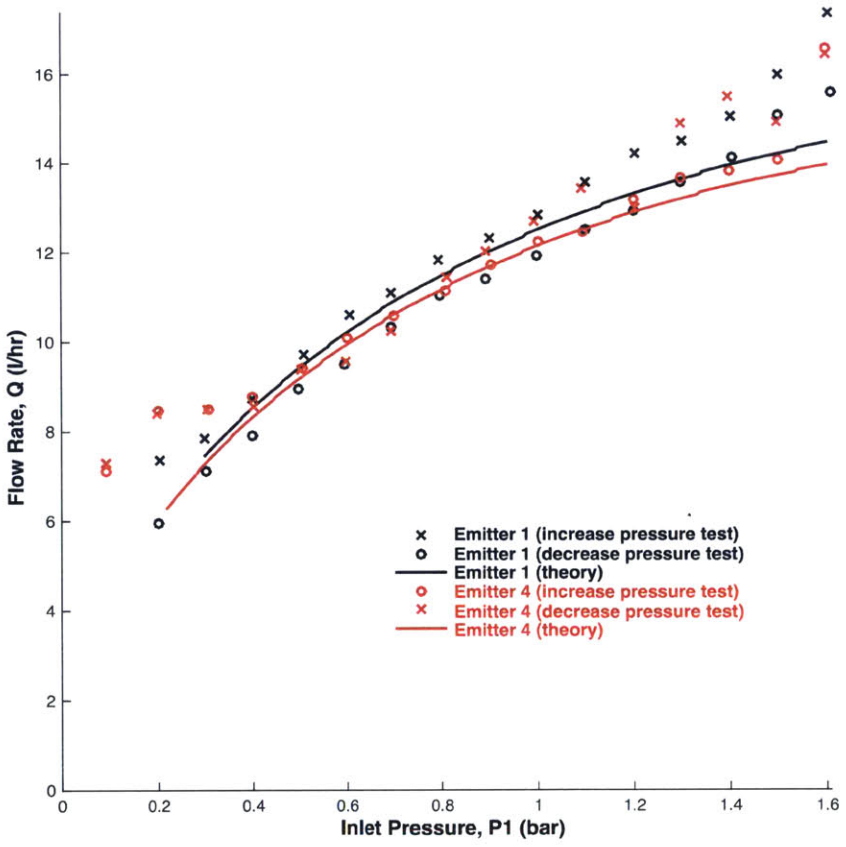

Figure 4-4: **Flow rate versus inlet pressure with variations in channel width.** Two CNC milled emitters were tested simultaneous, and the tests repeated five times for increasing and decreasing pressures tests. The plotted results are averages from the 10 data set each.

Length of Channel Figure 4-5 shows a close correlation between the experimental data and theoretical predictions for differing channel lengths. The results for emitter 5 have an R^2 value of 0.94. The trend seen is that an increase in channel length does not influence the flow rate versus pressure graph for the pressure range tested. This can be explained by the fact that the effective channel length (length of channel sealed by the membrane) does not vary at the pressures tested, hence there is no change in flow resistance. If the effective length did increase, the trend would be a lower flow rate. This trend is seen in industry, where tortuous paths are sometimes used under the flexible membrane to increase the effective channel length [2, 50].

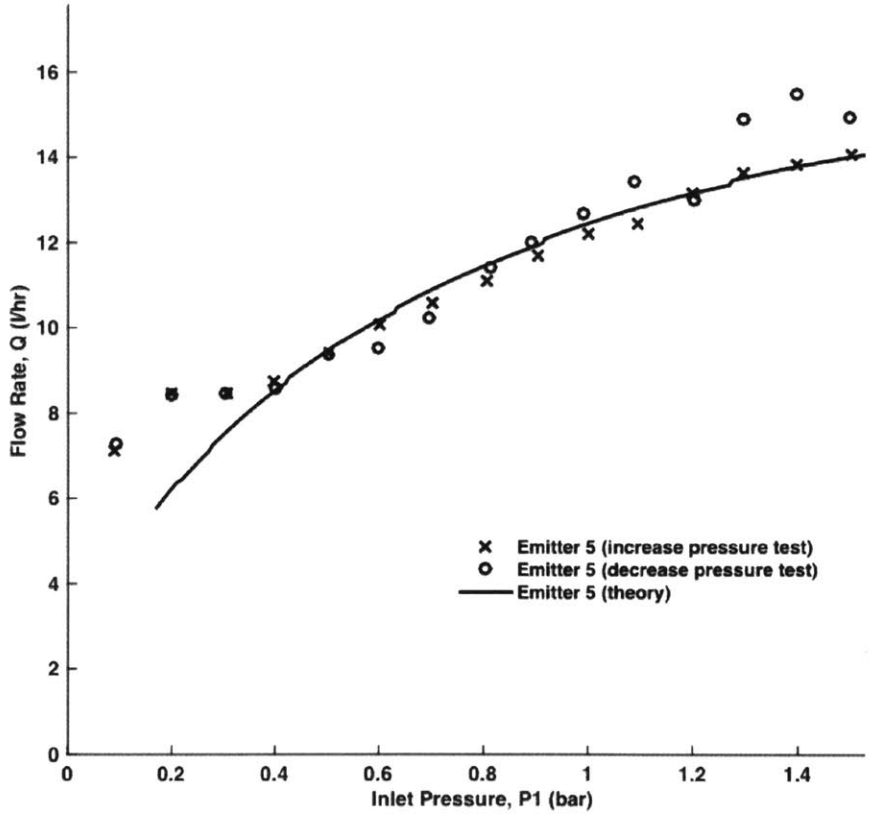

Figure 4-5: **Flow rate versus inlet pressure with variations in channel length.** Two CNC milled emitters were tested simultaneous, and the tests repeated five times for increasing and decreasing pressures tests. The plotted results are averages from the 10 data set each.

Deflection to Lands Figure 4-6 shows a close correlation between the experimental data and theoretical predictions for differing land heights. Emitter 6 has a R^2 value of 0.90. The trend seen is that a decrease in deflection height of the membrane led to a decrease in flow rate. This is because for the same pressure, a shorter deflection to the land results in a larger deformation in shear, hence a higher flow resistance.

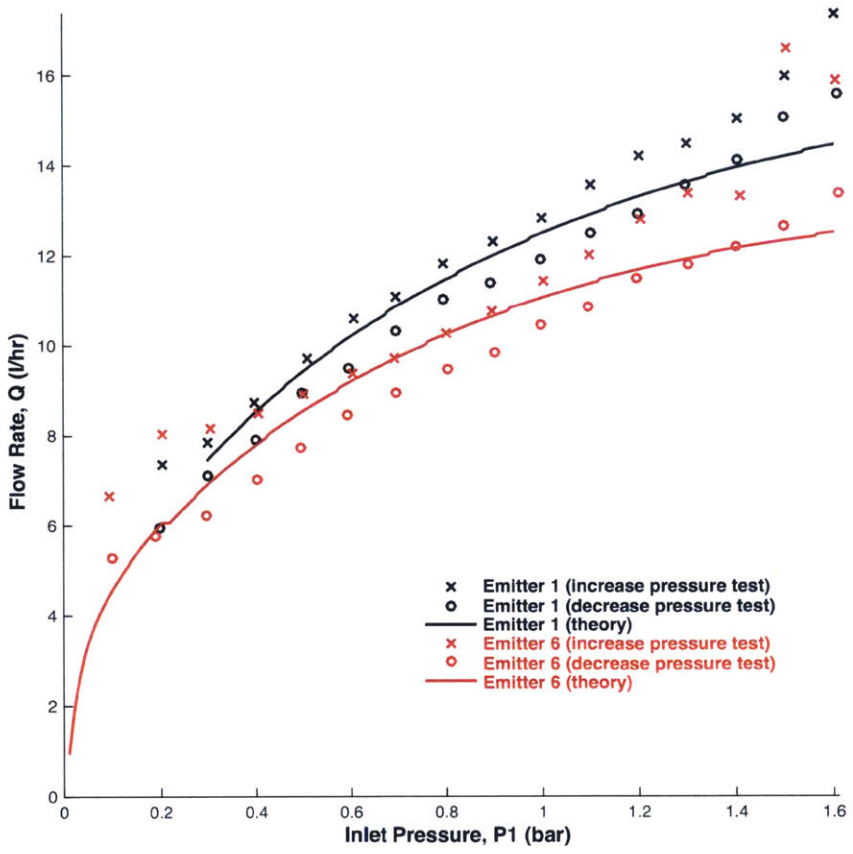

Figure 4-6: **Flow rate versus inlet pressure with variations in the membrane deflection to the lands.** Two CNC milled emitters were tested simultaneous, and the tests repeated five times for increasing and decreasing pressures tests. The plotted results are averages from the 10 data set each.

Combination of Variables Figures 4-7 and 4-8 shows a close correlation between the experimental data and theoretical predictions for changing a combination of variables. Emitter 7 has a R^2 value of 0.90 and emitter 8 has a R^2 value of 0.85 but very closely follows the trend.

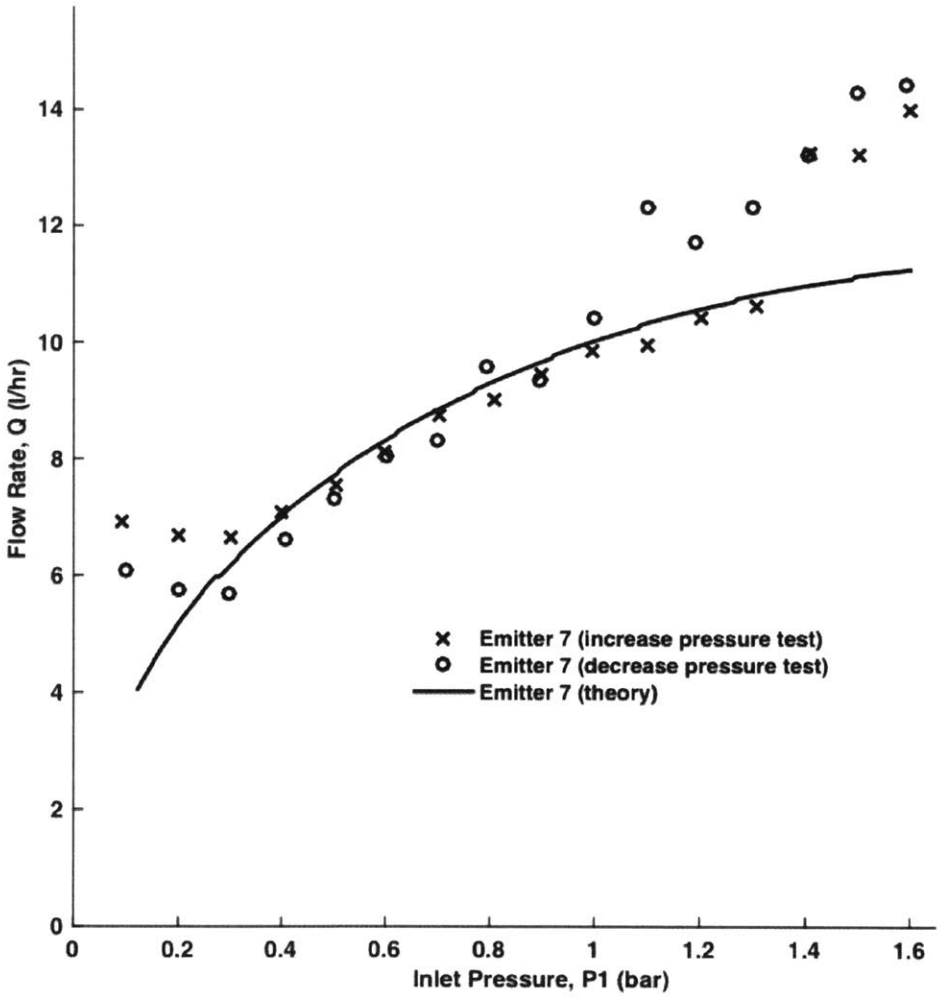

Figure 4-7: **Flow rate versus inlet pressure with variations in the membrane deflection to the lands.**Two CNC milled emitters were tested simultaneous, and the tests repeated five times for increasing and decreasing pressures tests. The plotted results are averages from the 10 data set each.

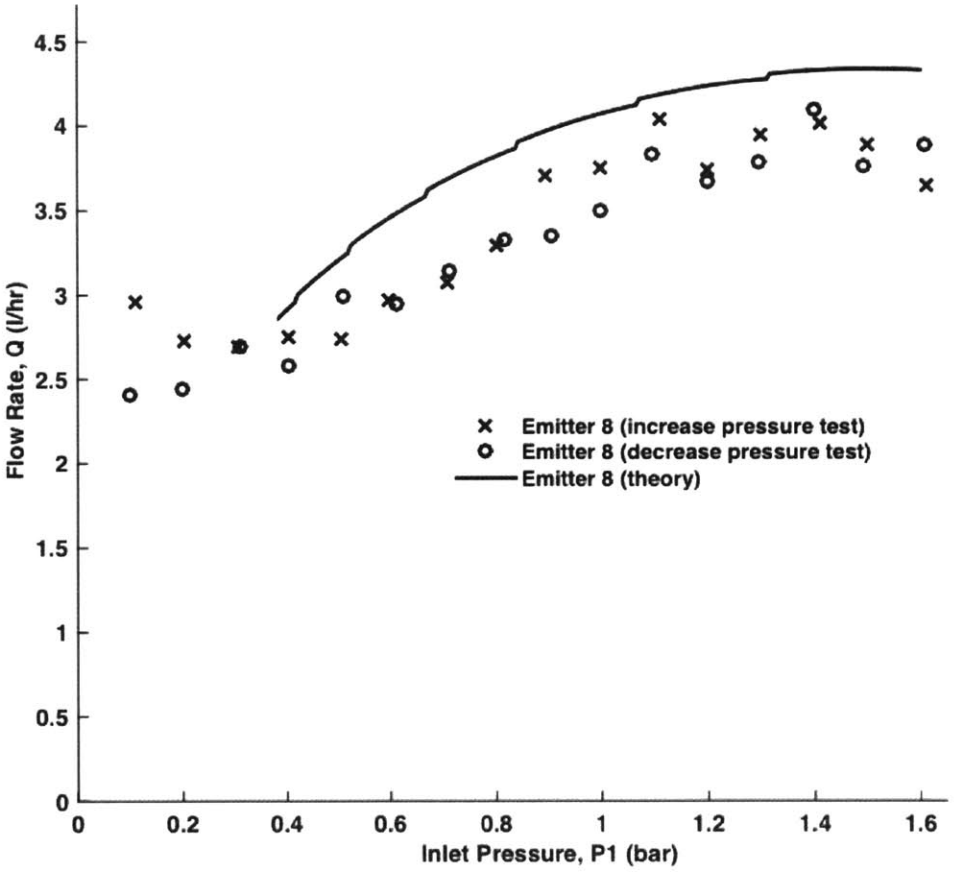

Figure 4-8: **Flow rate versus inlet pressure with variations in the membrane deflection to the lands.** Two CNC milled emitters were tested simultaneous, and the tests repeated five times for increasing and decreasing pressures tests. The plotted results are averages from the 10 data set each.

4.2 Single Objective Genetic Algorithm

The experimentally validated FSI model can be used to compute the flow rate versus inlet pressure curve for a particular geometry based on variables in emitter geometry such as, channel depth, width, length, the outlet diameter, the maximum height of deflection, the size of the orifice and the diameter and thickness of the compliant membrane. This model is capable of determining the flow rate versus pressure graph for a given architecture of the emitter within a $\pm$ 5% error bound. This model was used to conduct a hybrid genetic algorithm (GA) based [51] optimization study. Hybrid GA's combine the power of a GA with human intuition for decision making. The GA portion excels at narrowing the design space towards a global minimum but tends to slow down as it approaches the minimum. At this stage, human intuition is used to refine the search. The following final parameters were set based on prior experiments to conduct the optimization study using the GA optimization toolbox in MATLAB.

1. Population size = 100
2. Mutation rate = 0.03
3. Crossover rate = 0.8
4. Maximum generation = 20
5. Stopping conditions was set as follows: The deviation between the graphs (aimed versus design) is less than 5% OR the algorithm runs for 20 generations

Once the iterations came to a stop, human intuition was used used to achieve a better fit.

4.2.1 8.2 litre per hour emitter

The described procedure was followed to optimize an emitter of 8.2 lph. The result of this process is a set of optimal values for the set of input design variables described during Problem Formulation. I am presenting the results from a validation study conducted in conjunction with the project sponsor to characterize our optimal design. For this, we manufactured a Delrin emitter based on the optimal design for the 8 lph emitter. This emitter was experimentally tested using the procedure described in experimental protocol. Results from this experiment are shown in Figure 4-10. These results indicate that the optimized design had an activation pressure of 0.15 bars. This is significantly lower than the activation pressure for the original emitter design of 1 bar.

To independently confirm the lab-results for the 8.2 lph emitter, the project sponsor manufactured 50 HDPE emitters at their industrial facility. These emitters were injection molded without significant added costs as a result of the manufacturing constraints set during the problem formulation stage. The tests conducted conformed to ISO guidelines for testing PC emitters. Figure 4-9 shows how the performance of the optimized 8.2 lph emitters (labelled MIT) when compared to other current emitters. The optimized emitter has an activation pressure of 0.15 bar. This value is close to approximately $\frac{1}{6}^{\text{th}}$ of the activation pressure measured in other commercial designs.

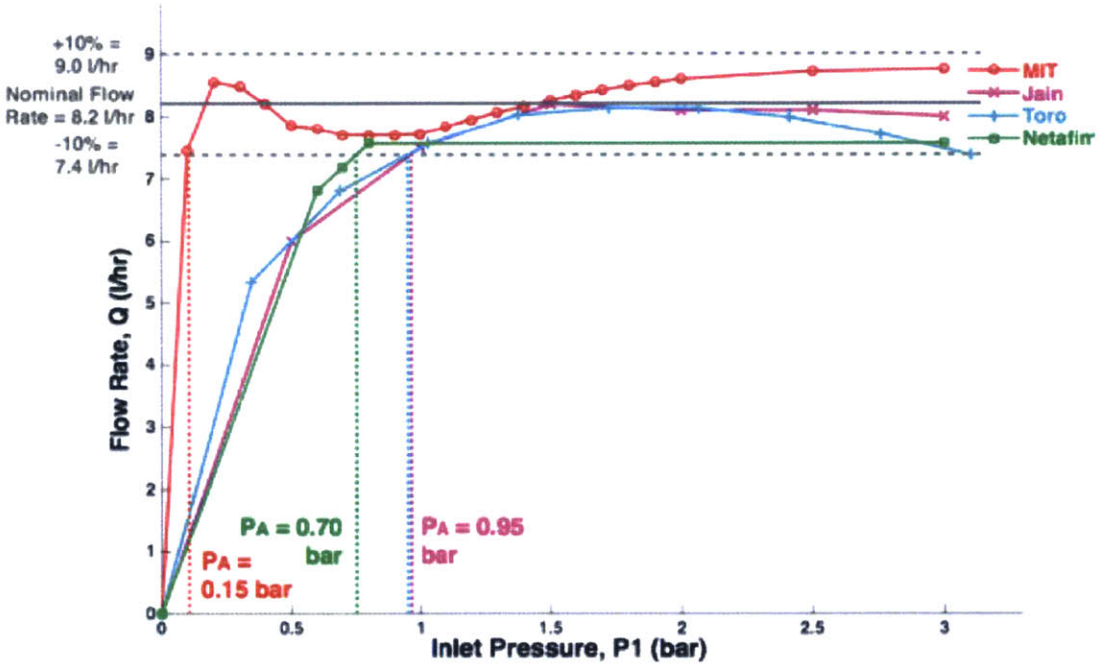

Figure 4-9: **Flow rate versus inlet pressure for optimized emitter (MIT) when compared to commercially available 8.2 lph emitters.** The number of MIT designed emitters tested at Jain is 50. The optimized emitter (MIT) is depicted in red and has an activation pressure that is 5 times lower than that of Netafim and 6 times lowers than Toro and Jain.

4.2.2 Family of Emitters

Experimental studies on optimal designs for emitters with flow rates of 4,6, and 7 lph obtained from the hybrid GA-based approach were also performed. Emitters with the optimized geometries were precision machined and tested at GEAR Lab, MIT. As shown in Figure 4-10, we observed an activation pressure of pressure of 0.2 bar or lower for all of these models. These results helped us confirm that applicability of our optimization approach across emitter architectures with varying flow rates. The numerical values for the different design variables that allowed the realization of lowering the activation pressure while also having a family of flow rates can be found in the Patent by Shamshery et al. (US Patent- 62/258067)- Pressure Compensating Emitter Having Very Low Activation Pressure and Large Operating Range.

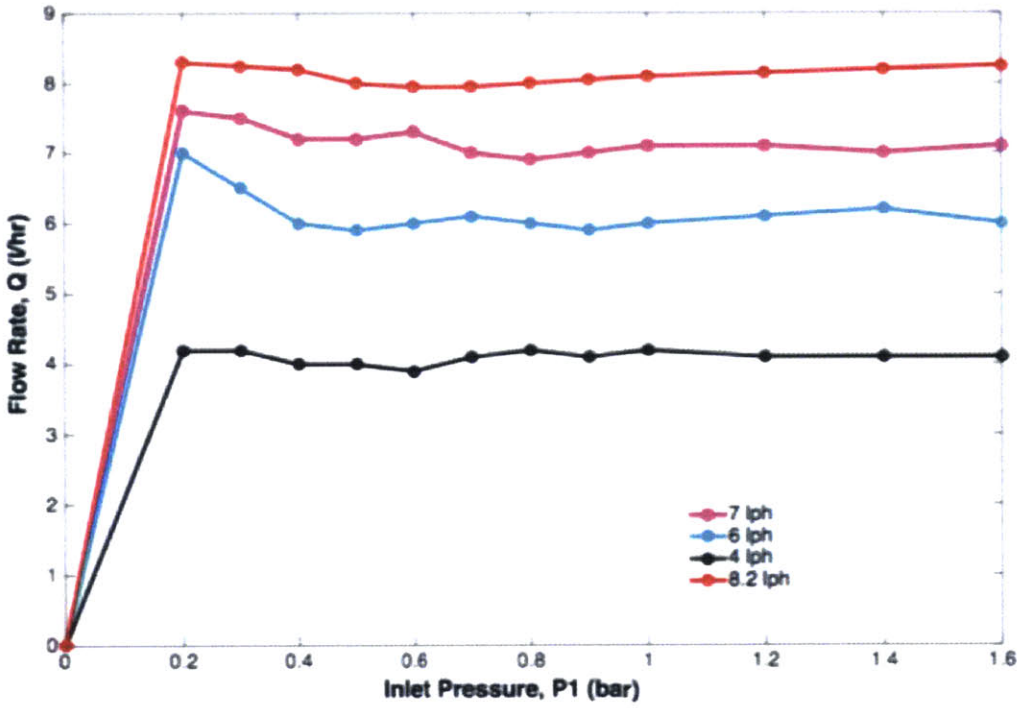

Figure 4-10: **Flow rate versus inlet pressure for emitters that were optimized using a hybrid GA and the model presented in this study.** Two CNC milled emitters were tested simultaneous, and the tests repeated five times while increasing and decreasing pressures. The plotted results are averages from the 10 data set each. They all have an activation pressure of 0.2 bar and lower.

Chapter 5

Conclusions and Future Work

5.1 Challenge

The global community, and India in particular, is facing an increasingly serious crisis with regards to the food-energy-agriculture nexus. In order to feed a growing population, shifting towards a more nutritious and water intensive diet on dwindling water and energy stressed resources, shifts will have to be made to more water and energy efficient methods of irrigation. Drip irrigation is an excellent candidate for sustainable agricultural development because it can increase crop yields by up to 50% while decreasing water consumption per acre by up to 70%, compared to traditional flood irrigation systems. The main inhibitor to the widespread adoption of drip is the high initial investment costs. A drip system costs $1000 an acre and an additional $3000 for solar.

5.2 Approach

Performing a cost analysis on the off-grid drip irrigation systems revealed that approximately 80 - 86% of the cost for drip systems with either PC 1 bar activation pressure or NPC emitters stems from the powering and pumping system. A reduction in the cost of these systems will result in a significant reduction of the cost of the overall off- grid drip system.

A reduction in the system pressure requirement would result in a reduction of power requirement and hence take a step towards reducing the overall cost of the system. A pressure loss analysis showed that the activation pressure of a 1 bar PC emitter accounts for 64% of the total pressure drop. If this loss can be reduced to 0.15 bar, this will reduce the pressure loss in the drip system by 55% and lead to a reduction in costs of an off-grid drip irrigation system by 50% from an average of $4000/acre to $2000/acre with the majority of the cost reduction occurring due to the reduction in CAPEX of solar panels.

5.3 Analysis

Prior art of emitters was looked into and to my knowledge, there is no existing study that analytically describes the principal operating characteristics and geometric dependence of PC drip emitters. At present, emitter design is guided by designers' empirical intuition and iterative experimentation, or by computer-aided emulation. The iterative method leads to designs at local optimums and the computer-aided emulation is difficult and time consuming to perform sensitivity analysis on and gain key insights into how the operation is dependent on geometry and materials. This is surprising given that one of the first patents for PC emitters was obtained in 1949, and the architecture of currently manufactured emitters very closely resembles this design.

This thesis presented a novel parametric fluid-structure interaction analysis on a currently manufactured 8.2 lph emitter. This parametric 2D model was validated using existing and currently manufactured Jain's 8.2 lph emitters as well as 8 different geometries CNC machined emitters. The model is capable of outputting the performance metric of an emitter, the flow rate versus pressure graph, for any input geometry within the constraints. This model was then coupled with a genetic algorithm to optimize the 8.2 lph emitter to have a low activation pressure, as low as 0.15 bar. The GA coupled model was also utilized to realize a family of emitters with flow rates of 4, 6, 7 and 8.2 lph while having an activation pressure of 0.2 bar and lower.

5.4 Results

The optimised 8.2 lph dripper was CNC machined at MIT (5 duplicate copies) and tested in the lab to reveal an activation pressure of 0.15 bar. To independently confirm the lab-results for the 8.2 lph emitter, the project sponsor manufactured 50 HDPE emitters at their industrial facility. These emitters were injection molded without significant added costs as a result of the manufacturing constraints set during the problem formulation stage. The tests conducted conformed to ISO guidelines for testing PC emitters. The optimized emitter was concluded to have an activation pressure of 0.15 bar. This value is close to 22% of the activation pressure measured in other commercial designs.

The family of other flow rates 4, 6 and 7 have been tested at MIT (5 duplicate copies each) and revealed an activation pressure of 0.2 or lower.

The model and design techniques presented here can be used to optimise PC online drippers for an flow rate with an activation pressure of 0.2 bar or lower. The new design methodology of optimizing emitters can be applied to any emitter, online and inline alike.

The design methodology consists of four main steps. First and most importantly, understand the fluid structure interaction with the emitter. Each different architecture will require a new model. Second is to validate the parametric model with existing benchmark emitters and other manufactured emitters. Third is to couple the model with an optimization toolbox in order to achieve a reduction in activation pressure. Lastly, is to validate the results from the GA. For a similar architecture, the last two steps can be iterated to optimize a family of different flow rate emitters.

5.5 Future Work

5.5.1 Emitter

The next step in the emitter research is to follow the verified design methodology to optimize a family of inline emitters. This will be done in two steps, firstly optimizing

existing portfolio of inline emitters and then inventing a new architecture in order to reduce the cost of emitter while achieving low activation PC behavior. This direction is being targeted by another Master's student in the Global Engineering and Research (GEAR) Lab.

5.5.2 System Level Optimization

Optimizing a PC emitter leads to a significant reduction in the overall cost of an off- grid system, but the optimized cost of $2000/acre is still too high. This system level optimization has two main objectives. The main aim of this study is to identify the sensitivities of different parameters and design variables to the overall cost of the system. Another objective is to identify the key technological advancements required in order to take a step towards making drip irrigation systems economically accessible to smallholder farmers. It should also be noted that a reduction in activation pressure leads to an optimized system curve. In order to realize the benefit of lower activation pressure an assumption has been made that a low- pressure pump exists. Further research would need to be done to find or redesign such a pump.

5.6 Key Contributions

The key contributions to research and irrigation presented in this thesis can be divided into three main classes:

1. **2D Parametric FSI model**

   As was noted earlier, to my knowledge, there is no existing study that analytically describes the principal operating characteristics and geometric dependence of PC drip emitters. This is a novel model that utilizes existing fluid and structure theory to model the compliant membrane deformation and fluid flow as a function of the dimensions of the architecture. The model is capable of outputting the performance metric of an emitter, the flow rate versus pressure graph, for any input geometry within the constraints. This parametric 2D

model was validated using existing and currently manufactured Jain's 8.2 lph emitters as well as 8 different geometries CNC machined emitters. This model can be coupled with a genetic algorithm to optimize a family of online emitters with a similar architecture.

2. **Emitter design metholody**

   The design methodology consists of four main steps. First and most importantly, understand the fluid structure interaction with the emitter. Each different architecture will require a new model. Second is to validate the parametric model with existing benchmark emitters and other manufactured emitters. Third is to couple the model with an optimization toolbox in order to achieve a reduction in activation pressure. Lastly, is to validate the results from the GA. For a similar architecture, the last two steps can be iterated to optimize a family of different flow rate emitters. The new design methodology of optimizing emitters can be applied to any emitters, online and inline alike.

3. **Optimized emitters**

   Jain Irrigation manufactured 50 of the optimized 8.2 lph HDPE emitters at their industrial facility. These emitters were injection molded without significant added costs as a result of the manufacturing constraints set during the problem formulation stage. The tests conducted conformed to ISO guidelines for testing PC emitters. The optimized emitter was confirmed to hav an activation pressure of 0.15 bar. This value is close to 22% of the activation pressure measured in other commercial designs.

   Using the above described methodology, a family of three other emitter flow rates (4,6 and 7) have been found to achieve an activation pressure of 0.2 bar or lower in the lab at MIT.

THIS PAGE INTENTIONALLY LEFT BLANK

Bibliography

[1] Irrigation in Southern and Eastern Asia in Figures - AQUASTAT Report. Technical report, FAO, 2004.

[2] Jain PC dripper Technical Datasheet. Available from: http://jisl.co.in/PDF/Catalogue_2015/drip/Drippers/j_sc_pc_plus_emitter.pdf. Last accessed on 15th May 2016.

[3] Wesley G Miller. Flow contol device US Patent 2,607,369, 1952.

[4] All India Report on Number and Area of Operational Holdings. Technical report, Government of India Agriculture Census 2010- 11, 2014.

[5] R.B. (FAO) Singh, P. (FAO) Kumar, and T. (FAO) Woodhead. Smallholder Farmers in India: Food Security and Agricultural Policy. Technical report, FAO.

[6] Agriculture, value added (annual % growth). The World Bank. http://data.worldbank.org/indicator last accessed on 24th February 2016.

[7] World Population Prospects. Elaboration of data by UN, Department of Economic and Social Affairs, Population Division. http://www.worldometers.info/world-population/india-population/ last accessed on 15th May 2016.

[8] Xavier Irz, Lin Lin, Colin Thirtle, and Steve Wiggins. Agricultural Productivity Growth and Poverty Alleviation Theoretical expectations of the effects of agricultural growth on poverty. In *Development Policy Review*, volume 19, pages 449–466. Blackwell Publishers, 2001.

[9] Luc Christiaensen, Lionel Demery, and Jesper Kuhl. The (Evolving) Role of Agriculture in Poverty Reduction. 2010.

[10] Investing in Smallholder Agriculture for Food Security. A Report by the High Level Panel of Experts on Food Security and Nutrition of the. Technical Report June, Committee on World Food Security, 2013.

[11] Smallholders, food security and the environment. Technical report, IFAD and UNEP, 2013.

[12] Dynamic Ground Water Resources of India. Technical Report March 2011, Central Ground Water Board Ministry of Water Resources, River Development& Ganga Rejuvenation, Government of India, 2014.

[13] John Briscoe and R.P.S Malik. *India's Water Economy: Bracing for a Turbulent Future.* Number 10. Oxford University Press, 2008.

[14] Tushaar Shah. The Groundwater Economy of South Asia: An Assessment of Size, Significance and Socio- ecological Impacts. In *The Agricultural Groundwater Revolution: Opportunities and Threats to Development*, chapter 2. 2007.

[15] Deep Wells and Prudence : Towards Pragmatic Action for Addressing Groundwater Overexploitation in India. Technical report, The International Bank for Reconstruction and Development/The World Bank, 2010.

[16] McKinsey & Company. Charting Our Water Future, Economic frameworks to inform decision- making. Technical report, McKinsey & Company The International Finance Corporation The Barilla Group The Coca-Cola Company, 2009.

[17] Evaluation Report on Rajiv Gandhi Grameen Vidyutikaran Yojana (RGGVY). Technical Report 224, Programme Evaluation Organisation Planning Commission Government of India, New Delhi, 2014.

[18] Natalie Obiko Pearson. India Approves 3 Billion Rupees in Solar Pump Subsidies. Available on: http://www.bloomberg.com/news/articles/2014-03-06/india-approves-3-billion-rupees-in-solar-pump-subsidies last accessed on 15th May 2016, 2014.

[19] National Mission on Micro Irrigation: Operational Guidelines. Technical report, Government of India Ministry of Agriculture Department of Agriculture & Cooperation, 2010.

[20] Pradhan Mantri Krishi Sinchayee Yojana, Andhra Pradesh Micro Irrigation Project. Available on: http:// horticulturedept.ap.gov.in/ Horticulture/ MIP/Farmer/ Category last accessed on 15th May 2016.

[21] National Mission on Micro Irrigation Government of Tamil Nadu. Available on: http://www.tn.gov.in/scheme/data/view/19378 last accessed on 15th May 2016.

[22] Department of soil & water conservation, Punjab. Available on: http:// dswcpunjab.gov.in /contents /micro/irrigation.htm last accessed on 15th May 2016.

[23] Micro- irrigation scheme, Gujarat Green Revolution Company Limited. Available on: http://ggrc.co.in/webui/Content.aspx?PageId=36 last accessed on 15th May 2016.

[24] Mazher Iqbal, Fayyaz-Ul-Hassan Sahi, Tamoor Hussain, Nasrullah Khan Aadal, Muhammad Tariq Azeem, and Muhammad Tariq. Evaluation Of Comparative Water Use Efficiency Of Furrow And Drip Irrigation Systems For Off-Season

Vegetables Under Plastic Tunnel. *International Journal of Agriculture and Crop Sciences*, 7(4):185–190, 2014.

[25] Regassa E. Namara, Bhawana Upadhyay, and R. K. Nagar. Adoption and Impacts of Microirrigation Technologies Empirical Results from Selected Localities of Maharashtra and Gujarat States of India. Technical report, International Water Management Institute, 2005.

[26] R. K. Sivanappan. Prospects of micro-irrigation in India. *Irrigation and Drainage Systems*, 8:49–58, 1994.

[27] Kamil Nkya, Amana Mbowe, and Joachim H J R Makoi. Low -Cost Irrigation Technology, in the Context of Sustainable Land Management and Adaptation to Climate Change in the Kilimanjaro Region. *Journal of Environment and Earth Science*, 5(7):45–56, 2015.

[28] Dinesh Kumar, Hugh Turral, Bharat Sharma, Upali Amarasinghe, and O. P. Singh. Water Saving and Yield Enhancing Micro Irrigation Technologies in India : When and where can they become best bet technologies? Technical Report September 2015, International Water Management Institute, 2008.

[29] Shilp Verma, S. Tsephal, and T. Jose. Pepsee systems: grassroots innovation under groundwater stress. *Water Policy*, 6(4):3003– 318, 2004.

[30] The irrigation challenge- Increasing irrigation contribution to food security through higher water productivity from canal irrigation systems. Technical report, Food and Agriculture Organization of the United Nations, Rome, 2003.

[31] K K Shashidhara, a Bheemappa, L V Hirevenkanagoudar, and K C Shashidhar. Benefits and constraints in adoption of drip irrigation among the plantation crop growers. *Karnataka Journal of Agricultural Sciences*, 20(1):82–84, 2007.

[32] D. Suresh Kumar. Adoption of Drip Irrigation System in India: Some Experience and Evidence. *Bangladesh Development Studies*, XXXV(1), 2012.

[33] A. Narayanamoorthy. Drip irrigation in India: Can it solve water scarcity? *Water Policy*, 6(2):117–130, 2004.

[34] Matthias Heil, Andrew L. Hazel, and Jonathan Boyle. Solvers for large-displacement fluid-structure interaction problems: Segregated versus monolithic approaches. *Computational Mechanics*, 2008.

[35] Hermann G. Matthies and Jan Steindorf. Partitioned strong coupling algorithms for fluid-structure interaction. *Computers and Structures*, 2003.

[36] Carlos A. Felippa, K. C. Park, and Charbel Farhat. Partitioned analysis of coupled mechanical systems. *Computer Methods in Applied Mechanics and Engineering*, 2001.

[37] K Bletzinger, T Gallinger, and A Kupzok. Partitioned Strategies for optimization in FSI. In *European Conference on Computational Fluid Dynamics*, 2006.

[38] Warren C. Young and R. J. Roark. *Roark's Formulas for Stress and Strain.* McGraw-Hill, New York, 2012.

[39] S Timoshenko and S Woinowsky- Krieger. *Theory of Plates And Shells.* McGraw-Hill Book, 1987.

[40] Y . M Ghugal and R Sharma. A refined shear deformation theory for flexure of thick beams. *Latin American Journal of Solids and Structures*, 8:183–195, 2011.

[41] J. Judy, D. Maynes, and B. W. Webb. Characterization of frictional pressure drop for liquid flows through microchannels. *International Journal of Heat and Mass Transfer*, 2002.

[42] Dorin Lelea, Shigefumi Nishio, and Kiyoshi Takano. The experimental research on microtube heat transfer and fluid flow of distilled water. *International Journal of Heat and Mass Transfer*, 2004.

[43] Jyh-Tong Teng. Fluid Dynamics in Microchannels. In *Fluid Dynamics, Computational Modeling and Applications*, pages 403–436. InTech, 2012.

[44] Mohsen Akbari, David Sinton, and Majid Bahrami. Pressure Drop in Rectangular Microchannels as Compared With Theory Based on Arbitrary Cross Section. *Journal of Fluids Engineering*, 131, 04 2009.

[45] W. M. Kays and A. L. London. *Compact Heat Exchangers.* McGraw- Hill, New York, 1984.

[46] Y. S. Muzychka and M. M. Yovanovich. Pressure Drop in Laminar Developing Flow in Noncircular Ducts: A Scaling and Modeling Approach. *Journal of Fluids Engineering*, 2009.

[47] Zhipeng Duan, M. M. Yovanovich, and Y. S. Muzychka. Pressure Drop for Fully Developed Turbulent Flow in Circular and Noncircular Ducts. *Journal of Fluids Engineering*, 2012.

[48] C Burt. Low-Pressure Testing Microirrigation Emitters. Technical report, Irrigation Training and Research Center, 2013.

[49] Indian Standard Irrigation Equipment, Emitters, Specification IS 13487. Technical report, Bureau of Indian Standards, 1997.

[50] Netafim PC dripper- Technical Datasheet. Available from: https://www.netafim.com/Data/Uploads/140815 PC dripper technical information_1.pdf last accessed on 15th May 2016.

[51] Randy L. Haupt and Sue Ellen Haupt. *Practical Genetic Algorithms.* Wiley, 2nd edition, 2004.